AD_____

Award Number: DAMD17-03-1-0531

TITLE: The Role of a Novel Topological Form of the Prion Protein in Prion Disease

PRINCIPLE INVESTIGATOR: Richard S. Stewart, Ph. D.

CONTRACTING ORGANIZATION: Washington University
St. Louis, MO 63110

REPORT DATE: July 2005

TYPE OF REPORT: Annual

PREPARED FOR: U.S. Army Medical Research and Materiel Command
Fort Detrick, Maryland 21702-5012

REPORT DOCUMENTATION PAGE

Form Approved
OMB No. 0704-0188

1. REPORT DATE	2. REPORT TYPE	3. DATES COVERED
01-07-2005	Annual	1 Jul 2004 – 30 Jun 2005

4. TITLE AND SUBTITLE

The Role of a Novel Topological Form of the Prion Protein in Prion Disease

5a. CONTRACT NUMBER

5b. GRANT NUMBER
DAMD17-03-1-0531

5c. PROGRAM ELEMENT NUMBER

6. AUTHOR(S)

Richard S. Stewart, Ph. D.

5d. PROJECT NUMBER

5e. TASK NUMBER

5f. WORK UNIT NUMBER

7. PERFORMING ORGANIZATION NAME(S) AND ADDRESS(ES)

Washington University
St. Louis, MO 63110

8. PERFORMING ORGANIZATION REPORT NUMBER

9. SPONSORING / MONITORING AGENCY NAME(S) AND ADDRESS(ES)
U.S. Army Medical Research and Materiel Command
Fort Detrick, Maryland 21702-5012

10. SPONSOR/MONITOR'S ACRONYM(S)

11. SPONSOR/MONITOR'S REPORT NUMBER(S)

12. DISTRIBUTION / AVAILABILITY STATEMENT
Approved for Public Release; Distribution Unlimited

13. SUPPLEMENTARY NOTES
Original contains colored plates: ALL DTIC reproductions will be in black and white.

14. ABSTRACT

Most(but not all) cases of prion disease are associated with a conformationally altered form of the prion protein (PrP) known as PrPSc. Several lines of evidence indicate that while PrpSc is the infectious molecule, it may not be the proximate cause of toxicity in prion disease. Several other candidates for such a toxic species have been proposed, including an altered topological form of PrP known as CtmPrP. Lines of transgenic mice engineered to express CtmPrP develop a spontaneous prion-like disease. Thus, extending our knowledge of the biology of CtmPrP will likely lead to important clues about how all prion diseases induce neurotoxicity. We have characterized the cell biology of CtmPrP in detail in cultured neurons, and show that its cellular trafficking differs from normal PrP. We have also learned that CtmPrP is much less toxic when expressed on a PrP null genetic background; this result has important implications for the mechanism of toxicity in prion disease. We have attempted to establish a cell culture model for CtmPrP-dependent toxicity to further define the mechanism of cell injury.

15. SUBJECT TERMS
Prions;Transmembrane PrP;transgenic mice;neurotoxicity

16. SECURITY CLASSIFICATION OF:				18. NUMBER OF PAGES	19a. NAME OF RESPONSIBLE PERSON
a. REPORT	b. ABSTRACT	c. THIS PAGE			USAMRMC
U	U	U	UU	26	19b. TELEPHONE NUMBER *(include area code)*

Standard Form 298 (Rev. 8-98)
Prescribed by ANSI Std. Z39.18

Table of Contents

INTRODUCTION

Prion diseases are commonly associated with the presence of a conformationally altered form of the prion protein (PrP^{Sc}). However, there is mounting evidence that PrP^{Sc} is not directly toxic to neurons; it may require interaction with other gene products to induce a neurotoxic program. Additionally, several PrP mutants have been studied in animal models which induce a neurodegenerative illness in most respects similar to experimental infection with prions, but do not make detectable PrP^{Sc} in their brains. One such alternate neurotoxic PrP species is ^{Ctm}PrP, which results from an alternate topological decision when the prion protein is translocated into the endoplasmic reticulum. ^{Ctm}PrP has also been proposed to be induced by experimental scrapie infection, which suggests that ^{Ctm}PrP may be the ultimate toxic trigger. We have identified mutations in the prion protein sequence which dramatically favor the production of ^{Ctm}PrP (which under normal conditions is not detectable). We have established lines of transgenic mice which express ^{Ctm}PrP [designated Tg(L9R-3AV)], and these mice develop a spontaneous neurological illness similar to scrapie. We are characterizing the phenotype of these mice to further our understanding of ^{Ctm}PrP–meditated neurotoxicity, which we believe will shed new light on the process of neurodegeneration in prion disease.

BODY

Task 1: Generation of anti-signal peptide antisera. Months 1-24.

We have previously shown that an antiserum raised against the signal peptide (SP) of PrP will specifically recognize ^{Ctm}PrP *in vitro* and in cultured cells [Stewart and Harris 2003]. The principle is that since ^{Ctm}PrP is a type II transmembrane protein, its N-terminal signal peptide will not be inserted into the ER lumen and be cleaved by signal peptidase, while PrPC is processed in this manner. We have used this serum to show that the prion protein encoded by our Tg(L9R-3AV) transgenic mice is recognized by this anti-SP antiserum, while non-transgenic controls are not recognized. We have further used this serum to look for the presence of CtmPrP in terminally ill scrapie-infected mice, and did not detect any ^{Ctm}PrP [Stewart and Harris 2003].
We have proposed creating monoclonal antibodies to the SP, but we have not proceeded with this goal, since the above results indicate that ^{Ctm}PrP is not produced at appreciable levels in infected animals.

Task 2: Characterization of the ^{Ctm}PrP-induced neurotoxic pathway *in vivo* and *in vitro*. Months 12-36.

We know that the granule cell layer of the cerebellum is the preferential target of toxicity induced by ^{Ctm}PrP production. We see massive loss of granule cells in terminally ill mice,

with lesser amounts of loss in the hippocampus. Preliminary data suggests this cell loss occurs at least in part through apoptotic mechanisms (as indicated by TUNEL staining). Perhaps the most surprising result from the transgenic mice is that the severity of the phenotype is markedly affected by the presence of the endogenous PrP gene (PrnP). The original Tg(L9R-3AV) lines (designated B and C) were created on a PrnP +/+ genetic background. The Tg(L9R-3AV) B/PrnP +/+ mice develop ataxia at 170 days, while Tg(L9R-3AV) B/PrnP o/o mice never develop illness (still healthy at 600 days) [Stewart et al 2005]. A less dramatic result was observed in the C line: Tg(L9R-3AV) C/PrnP +/+ mice get sick at 85 days, while Tg(L9R-3AV) C/PrnP o/o mice develop symptoms significantly later (145 days)[Stewart et al. 2005]. There is a more dramatic extension of the duration of illness in the Tg(L9R-3AV) C/PrnP o/o line (mice have been observed for over 400 days without progression to terminal illness, while Tg(L9R-3AV) C/PrnP +/+ mice are terminally ill by 150-180 days) [Stewart et al 2005]. We believe these results suggest a genetic interaction between ^{Ctm}PrP and PrP^{C}, and may yield new information toward the function of endogenous PrP (which is as yet unknown).

We have also begun to analyze the molecular mechanism of cell death in the brain by genetic analysis. The Bax protein is recognized as an important regulator of neuronal cell death both *in vitro* and *in vivo*. Previous studies in our laboratory have established a role for Bax function in the cerebellar granule cell death which occurs in transgenic mice expression the PG14 PrP mutation. Surprisingly, while Bax deletion rescued the cell death, it did not rescue the neurological phenotype of these mice [Chiesa et al. 2005]. This result suggests that neuronal dysfunction, rather than cell death *per se*, may be a key feature of prion disease. We have crossed the Tg(L9R-3AV) C/ PrnP +/+ mice to Bax null mice. Preliminary results suggest that a similar phenomenon occurs in these mice; neurological illness developed when expected, but neuronal loss was at least partially rescued. We will pursue these results further in the near future.

Establishment of a cell culture model for ^{Ctm}PrP–mediated toxicity would be a significant advance in the field, and would greatly facilitate the study of the molecular mechanism(s) of toxicity. We have extensively cultured cerebellar granule neurons from Tg(L9R-3AV) mice, but have not been able to demonstrate any greater susceptibility of these neurons to cell death in culture, despite the fact that we know these neurons die *in vivo*. Additionally, several insults which cause rapid cell death *in vitro* (such as potassium depletion or hydrogen peroxide treatment) do not show any preferential toxicity to Tg(L9R-3AV) neurons. Additionally, we have preformed exhaustive studies with CHO cells transfected with L9R-3AV PrP as well as other neurotoxic PrP mutants and have not been able to demonstrate reproducible PrP-dependent cell death. We have tentatively concluded that such a cell culture model may not be possible to establish, at least given our present understanding.

Task 3: Characterization of the cell biology of ^{Ctm}PrP. Months 37-48.

We have confirmed that Tg(L9R-3AV) mice produce ^{Ctm}PrP (and control mice do not) by several complementary approaches, including the anti-SP antibody described above. We have demonstrated by cell biological methods that neurons from Tg(L9R-3AV) mice produce ^{Ctm}PrP, and that the ^{Ctm}PrP in these neurons is localized to the Golgi apparatus [Stewart and Harris 2005]. We have confirmed this result is not an artifact of

the cell culture process by analyzing brain sections from Tg(L9R-3AV) mice by immunohistochemistry; they also show prominent ^{Ctm}PrP staining in the Golgi. The cell biology of ^{Ctm}PrP differs from that of PrP^{C}, and also differs from the cellular localization of the same mutant PrP expressed in CHO or BHK cells (where it is localized to the endoplasmic reticulum) [Stewart and Harris 2005]. The reason for this alternate localization in transfected cells remains unclear. We have also transfected L9R-3AV PrP into HpL cells (an immortalized neural cell line) and in this case it does localize to the Golgi, similar to the *in vivo* results. These results suggest that ^{Ctm}PrP may transmit its neurotoxic signal through the Golgi apparatus.

Task 4: Structure-function analysis of ^{Ctm}PrP using chimeric proteins. Months 42-60.

Not begun.

KEY RESEARCH ACCOMPLISHMENTS

- Tg(L9R-3AV) mice develop a spontaneous neurological illness with massive loss of cerebellar granule cells and accompanying gliosis.
- The illness in Tg(L9R-3AV) mice is at least partially dependent on the expression of endogenous PrP.
- The cell biology of CtmPrP differs considerably from endogenous PrP. CtmPrP is localized to the Golgi apparatus in Tg(L9R-3AV) mice and in certain cultured cell lines.
- Attempts to establish a cell-based assay for ^{Ctm}PrP-mediated toxicity were not successful.

REPORTABLE OUTCOMES

Publications:

Stewart, R. S., P. Piccardo, B. Ghetti, and D. A. Harris (2005). Neurodegenerative illness in transgenic mice expressing a transmembrane form of the prion protein. J. Neurosci. **25**: 3469-3477.

Stewart, R. S., and D. A. Harris (2005). A transmembrane form of the prion protein is in the Golgi apparatus of neurons. J. Biol. Chem. **280**:15855-15864.

Transgenic mouse lines:

Tg(L9R-3AV) B

Tg(L9R-3AV) C

CONCLUSIONS

We have established a model for a spontaneous neurodegenerative illness induced by an alternate topological isoform of PrP. We have shown that these mice do not produce any PrP^{Sc}. We have shown that the cell biology of ^{Ctm}PrP differs from PrP^{C}. We have demonstrated that the illness induced by ^{Ctm}PrP is partially dependent on the expression of endogenous PrP. We have attempted to establish a cell culture based model for ^{Ctm}PrP-mediated toxicity. Future work will focus on the role of endogenous PrP in the ^{Ctm}PrP-induced illness.

REFERENCES

Chiesa, R., P. Piccardo, S. Dossena, L. Nowoslawski, K.A. Roth, B. Ghetti, and D. A. Harris (2005). *Bax* deletion prevents neuronal loss but not neurological symptoms in a transgenic model of inherited prion disease. *Proc. Natl. Acad. Sci. USA* **102,** 238-243.
Stewart, R. S., P. Piccardo, B. Ghetti, and D. A. Harris (2005). Neurodegenerative illness in transgenic mice expressing a transmembrane form of the prion protein. J. Neurosci. **25**: 3469-3477.
Stewart, R. S., and D. A. Harris (2005). A transmembrane form of the prion protein is in the Golgi apparatus of neurons. J. Biol. Chem. **280**:15855-15864.
Stewart, R. S., and D. A. Harris (2003). Mutational Analysis of Topological Determinants in Prion Protein (PrP) and Measurement of Transmembrane and Cytosolic PrP during Prion Infection. J. Biol. Chem. **278**: 45960-45968.

APPENDICES

Publications

Neurobiology of Disease

Neurodegenerative Illness in Transgenic Mice Expressing a Transmembrane Form of the Prion Protein

Richard S. Stewart,[1] Pedro Piccardo,[2,3] Bernardino Ghetti,[2] and David A. Harris[1]

[1]Department of Cell Biology and Physiology, Washington University School of Medicine, St. Louis, Missouri 63110, [2]Division of Neuropathology, Indiana University School of Medicine, Indianapolis, Indiana 46202, and [3]Center for Biologics Evaluation and Research, Food and Drug Administration, Rockville, Maryland 20852

Although PrP^{Sc} is thought to be the infectious form of the prion protein, it may not be the form that is responsible for neuronal cell death in prion diseases. ^{Ctm}PrP is a transmembrane version of the prion protein that has been proposed to be a neurotoxic intermediate underlying prion-induced pathogenesis. To investigate this hypothesis, we have constructed transgenic mice that express L9R-3AV PrP, a mutant prion protein that is synthesized exclusively in the ^{Ctm}PrP form in transfected cells. These mice develop a fatal neurological illness characterized by ataxia and marked neuronal loss in the cerebellum and hippocampus. ^{Ctm}PrP in neurons cultured from transgenic mice is localized to the Golgi apparatus, rather than to the endoplasmic reticulum as in transfected cell lines. Surprisingly, development of the neurodegenerative phenotype is strongly dependent on coexpression of endogenous, wild-type PrP. Our results provide new insights into the cell biology of ^{Ctm}PrP, the mechanism by which it induces neurodegeneration, and possible cellular activities of PrP^{C}.

Key words: **prion; transgenic; neurodegeneration; Golgi; transmembrane; mutation**

Introduction

Prion diseases are associated with conformational conversion of an endogenous, neuronal glycoprotein (PrP^{C}) into an aggregated, β-sheet-rich isoform (PrP^{Sc}) that is infectious in the absence of nucleic acid (Prusiner, 1998; Weissmann, 2004). Because PrP^{Sc} accumulates in the brains of infected animals and humans, it has usually been assumed that this isoform is the cause of prion-induced neurodegeneration. However, several lines of evidence now suggest that, although PrP^{Sc} is the infectious form of PrP, it may not be the form directly responsible for neuronal death in prion diseases (for review, see Chiesa and Harris, 2001). Thus, there has been an attempt to identify the PrP species that initiate the neurodegenerative process. The present work focuses on one candidate for such a neurotoxic form of PrP, designated ^{Ctm}PrP.

PrP can be synthesized in the endoplasmic reticulum (ER) in three topological forms, designated ^{Sec}PrP, ^{Ntm}PrP, and ^{Ctm}PrP. ^{Sec}PrP molecules are attached to the outer leaflet of the lipid bilayer exclusively by a C-terminal glycosyl-phosphatidylinositol (GPI) anchor. ^{Ntm}PrP and ^{Ctm}PrP molecules span the lipid bilayer via a central hydrophobic region (amino acids 111–134), with either the N terminus or C terminus, respectively, on the extracytoplasmic side of the membrane (Hegde et al., 1998b; Hölscher et al., 2001; Kim et al., 2001; Stewart et al., 2001). ^{Ctm}PrP has been hypothesized to be a key pathogenic intermediate in both familial and infectiously acquired prion diseases (Hegde et al., 1999). In support of this proposition, transgenic mice expressing PrP with ^{Ctm}PrP-favoring mutations develop a scrapie-like neurological illness, but without PrP^{Sc} (Hegde et al., 1998b, 1999). However, a general role for ^{Ctm}PrP in prion diseases has been called into question by recent observations (Stewart and Harris, 2001, 2003), leaving the biological significance of this form unresolved.

A major difficulty in studying ^{Ctm}PrP is that it has not been possible to synthesize this form in either cultured cells or brain in the absence of the other two topological variants (^{Ntm}PrP and ^{Sec}PrP). To overcome this limitation, we identified nonconservative mutations in the hydrophobic core of the PrP signal peptide that markedly increased the proportion of ^{Ctm}PrP (Stewart et al., 2001; Stewart and Harris, 2003). Combining one of these mutations (L9R) with 3AV, a mutation within the transmembrane domain, to create L9R-3AV resulted in a protein that was synthesized exclusively as ^{Ctm}PrP, in both *in vitro* translation reactions and transfected cells (Stewart et al., 2001). The availability of L9R-3AV PrP provided us with the ability to analyze the properties of ^{Ctm}PrP in a cellular context in the absence of the other two topological variants (Stewart et al., 2001).

In the present study, we report on transgenic mice that express PrP carrying the L9R-3AV mutation. These Tg(L9R-3AV) mice develop a severe neurological illness accompanied by marked neuronal degeneration in several brain areas. Unexpectedly, we find that this phenotype is strongly dependent on coexpression of

Received Oct. 29, 2004; revised Feb. 15, 2005; accepted Feb. 16, 2005.

This work was supported by Department of Defense Grant DAMD-03-0531 (R.S.S.) and National Institutes of Health Grants NS40975 (D.A.H.) and P30 AG10133 (B.G.). No official endorsement of this article by the Food and Drug Administration is intended or should be inferred. We thank Charles Weissmann for *Prn-p*$^{0/0}$ mice, Richard Kascsak for 3F4 antibody, and Man-Sun Sy for 8H4 and 8B4 antibodies. We are grateful to Cheryl Adles and Michelle Kim for mouse colony maintenance and genotyping and to Rose Richardson and Constance Alyea for preparing histological specimens. We thank Mike Green for critically reading this manuscript.

Correspondence should be addressed to Dr. David A. Harris, Department of Cell Biology and Physiology, Washington University School of Medicine, 660 South Euclid Avenue, St. Louis, MO 63110. E-mail: dharris@cellbiology.wustl.edu.

DOI:10.1523/JNEUROSCI.0105-05.2005

 0270-6474/05/253469-09$15.00/0

endogenous, wild-type PrP. Our results have important implications for the cell biology of ^{Ctm}PrP, the mechanism by which it induces neurodegeneration, and possible physiological functions of PrP^{C}.

Materials and Methods

Transgenic mice. Construction of a plasmid that encodes mouse PrP containing the L9R-3AV mutation and the 3F4 antibody epitope (see Fig. 1) has been described previously (Stewart et al., 2001). The coding region of this plasmid was amplified by PCR using the following primers: GACCAGCTCGAGATGGCGAACCTTGGCTACTGG (sense); GACCAGCTCGAGTCATCCCACGATCAGGAAGAT (antisense). The amplified PCR product was digested with *Xho*I and inserted into the MoPrP.Xho vector (Borchelt et al., 1996). Purified DNA was injected into pronuclei of fertilized eggs from an F_2 cross of C57BL/6J × CBA/J F_1 parental mice. Founder animals were identified by PCR amplification of tail DNA using the following primers: AACCGAGCTGAAGCATTCTGCC (sense); CACGAGAAATGCGAAGGAACAAGC (antisense). Founders were bred to C57BL/6J × CBA/J (*Prn-p*$^{+/+}$) mice or to *Prn-p*$^{0/0}$ mice obtained from Charles Weissmann (Scripps Research Institute, West Palm Beach, FL). The latter mice, which were created on a C57BL/6J/129 background (Büeler et al., 1992), have been maintained in our laboratory by crossing onto the C57BL/6J × CBA/J background. For one line (B), transgenic animals were intercrossed to obtain progeny that were homozygous for the transgene array. The latter animals were identified by quantitative PCR. Tg(WT-E1)/*Prn-p*$^{0/0}$ and Tg(PG14-A2)/*Prn-p*$^{0/0}$ mice have been described previously (Chiesa et al., 1998). The transgenically encoded PrP in both of these lines carries the 3F4 epitope.

Animals were scored as ill if they displayed ataxia on a horizontal grid test (Chiesa et al., 1998), and they were considered to be terminal and were killed when they could no longer walk or feed themselves.

Histological analysis. Brain tissue was fixed, processed, and sectioned sagittally as described previously (Chiesa et al., 1998). Tissue sections were stained with hematoxylin and eosin. For detection of GFAP, sections were stained with an antibody from Biogenex (San Ramon, CA) at a 1:50 dilution, followed by visualization using the peroxidase–antiperoxidase (PAP) method with goat anti-rabbit IgG and rabbit PAP (Sternberger Monoclonals, Baltimore, MD). 3,3′-Diaminobenzidine was used as a chromogen. Sections were counterstained lightly with hematoxylin to reveal the localization of the cells.

Western blotting. Brain tissue was homogenized using a Teflon pestle in 10 vol of PBS containing protease inhibitors (in μg/ml: 20 PMSF, 10 leupeptin, and 10 pepstatin). Homogenates were clarified by centrifugation at 2000 × *g* for 5 min. Cultured neurons were lysed in 0.5% SDS and 50 mM Tris-HCl, pH 7.5, and the lysates were heated at 95°C for 10 min. Protein was quantified using a BCA assay (Pierce, Rockford, IL). Samples were analyzed by SDS-PAGE followed by immunoblotting with 3F4 antibody (Bolton et al., 1991) or 8H4 antibody (Zanusso et al., 1998).

Reverse transcriptase-PCR. RNA was extracted from freshly dissected forebrain or cerebellum using RNAWiz (Ambion, Austin, TX) according to the manufacturer's instructions. RNA was reverse transcribed and amplified in a one-step reaction using the Titanium kit (Clontech, Palo Alto, CA). The primers used to detect mRNA encoding transgene-derived PrP were CGCTGCGTCGCATCGGTGG (sense) and GCCATCTCGAGGTACCAC (antisense). The primers used to detect mRNA encoding endogenous PrP were GCCAAGCAGACTATCAG (sense) and CGGCTGTAGTCAGGTGTATCA (antisense). Mouse β-actin primers supplied by the manufacturer were included as an internal standard to correct for RNA input. Samples were removed every four cycles and analyzed on 8% polyacrylamide/Tris-borate EDTA gels. DNA band intensities were quantified by staining gels with SYBRGreen (Molecular Probes, Eugene, OR) and imaging with a Storm 860 phosphorimager (Amersham Biosciences, Arlington Heights, IL). The data shown were from those samples in which band intensities for both PrP and actin were within the linear range of amplification (generally 18 cycles).

Culturing and metabolic labeling of cerebellar granule cells. Primary cultures from 5-d-old pups were prepared as described previously (Miller and Johnson, 1996). Dissociated cells were resuspended in cerebellar granule neuron (CGN) medium (basal medium Eagle's, 10% dialyzed fetal bovine serum, 25 mM KCl, 2 mM glutamine, and 50 μg/ml gentamycin) and plated at a density of 500,000 cells/cm^2 in polylysine-coated plastic plates or 8-well glass chamber slides. Cells were used after 4–5 d in culture. These cultures contained >95% neurons, as assessed by staining with antibody to GFAP.

Cerebellar granule cells were labeled with 200 μCi/ml ^{35}S-Promix (Amersham Biosciences) in CGN medium lacking methionine, cysteine, and bovine serum and containing vitamin B27 supplement (Invitrogen, Carlsbad, CA). Cells were lysed in 0.5% SDS and 50 mM Tris-HCl, pH 7.5, and immunoprecipitation of PrP was performed as described previously (Drisaldi et al., 2003) using 3F4 or 8H4 antibody.

PrP membrane topology assay. Metabolically labeled cells were scraped with a pipette tip into PBS, spun at 2000 × *g* for 5 min, and resuspended in ice-cold homogenization buffer (in mM: 250 sucrose, 5 KCl, 5 $MgCl_2$, and 50 Tris-HCl, pH 7.5). Cells were lysed by 12 passages through SILASTIC tubing (inner diameter, 0.3 mm) connecting two syringes with 27 gauge needles, and nuclei were removed by centrifugation at 5000 × *g* for 10 min. Aliquots of the postnuclear supernatant were diluted into 50 mM Tris-HCl, pH 7.5, and incubated for 60 min at 4°C with 250 μg/ml proteinase K (PK) in the presence or absence of 0.5% Triton X-100. Digestion was terminated by the addition of PMSF (5 mM final concentration), and PrP was immunoprecipitated with 3F4 antibody and deglycosylated by treatment with peptide-*N*-(acetyl-β-glucosaminyl)-asparagine amidase (New England Biolabs, Beverly, MA).

Immunofluorescent labeling of brain sections and cultured neurons. Mice were perfused transcardially with 4% paraformaldehyde, after which the brains were postfixed for 3 h in the same solution and transferred to 0.1 M sodium phosphate, pH 7.2. Vibratome sections (50 μm) were incubated in blocking solution (PBS plus 2% goat serum and 0.2% Triton X-100) and stained with anti-PrP antibody 8B4 (Zanusso et al., 1998) and anti-giantin antibody (Covance, Berkeley, CA). Primary antibodies were visualized with a mixture of Alexa 488-coupled goat anti-mouse IgG and Alexa 594-coupled goat anti-rabbit IgG (Molecular Probes).

For surface labeling of cultured CGNs, cells were transferred to CGN medium containing vitamin B27 supplement instead of calf serum and stained in the living state for 10 min at 37°C with anti-PrP antibody 8H4. After rinsing with PBS, cells were fixed in 4% paraformaldehyde, 5% sucrose, and PBS for 10 min at room temperature and incubated in blocking solution (2% goat serum and PBS) for 10 min at room temperature. Cells were then stained with Alexa 488-coupled goat anti-mouse IgG, rinsed with PBS, and mounted in 50% glycerol and PBS. In some cases, cultures were incubated with phosphatidylinositol-specific phospholipase C (PIPLC) [final concentration, 1 U/ml; purified from *Bacillus thuringiensis* as described by Shyng et al. (1995)] before surface staining.

For internal labeling of cultured granule neurons, cells were fixed as above and permeabilized for 10 min at room temperature with 0.05% Triton X-100 in PBS. Cells were then incubated in blocking solution and stained with anti-PrP antibody 8B4 and anti-giantin antibody. Primary antibodies were visualized with a mixture of Alexa 488-coupled goat anti-mouse IgG and Alexa 594-coupled goat anti-rabbit IgG.

Cultured neurons and brain sections were viewed with a Zeiss (Oberkochen, Germany) LSM 510 confocal microscope equipped with an Axiovert 200 laser scanning system.

Assay of PrP^{Sc} properties. Cultures of cerebellar granule cells were labeled with ^{35}S-Promix as above. To assay detergent solubility, cells were lysed in buffer A (50 mM NaCl, 0.5% Triton X-100, 0.5% sodium deoxycholate, and 50 mM Tris-HCl, pH 7.5) at 4°C for 10 min. Lysates were first centrifuged at 14,000 × *g* for 10 min, and then the supernatant was centrifuged again at 180,000 × *g* for 40 min. PrP in supernatant and pellet fractions from the second centrifugation was immunoprecipitated and analyzed by SDS-PAGE.

To assay PK resistance, labeled cells were lysed in PK buffer (PBS plus 0.5% Triton X-100, 0.5% NP-40, 0.5% sodium deoxycholate, and 0.2% Sarkosyl), and the lysates were centrifuged at 10,000 × *g* for 10 min. Aliquots of the supernatant were treated with varying amounts of PK at 37°C for 20 min, and digestion was terminated by the addition of PMSF to a final concentration of 5 mM. PrP was then recovered by immunoprecipitation and analyzed by SDS-PAGE.

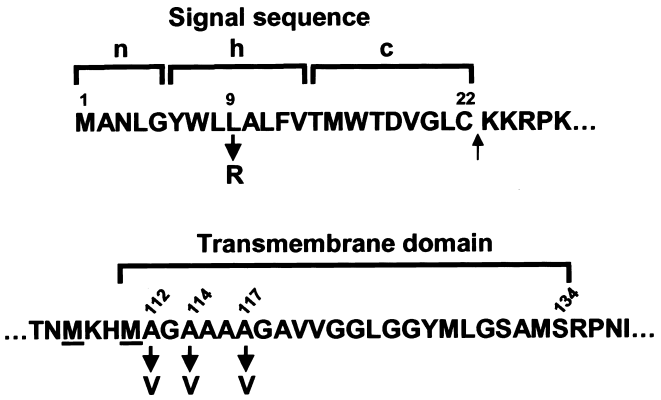

Figure 1. The amino acid sequence of murine PrP, with the L9R and 3AV mutations in the signal sequence and transmembrane domains, respectively, is shown. n, h, and c indicate, respectively, the N-terminal, hydrophobic, and C-terminal regions of the signal sequence. 3AV is the designation for the triple mutation A112V/A114V/A117V. The two underlined methionine residues at positions 108 and 111 were introduced to create an epitope for the 3F4 antibody, which allows discrimination of transgenically encoded and endogenous PrP. The upward arrow following residue 22 indicates the signal peptide cleavage site.

Table 1. Time course of neurological illness in Tg(L9R-3AV) mice

Line	Endogenous PrP (*Prn-p*)	Age at initial symptoms[a]	Age at death[a]	Number of animals
A/−	+/+	17 ± 2	21 ± 1	4[b]
B/−	+/+	172 ± 7	389 ± 12	26
B/−	0/0	>650	>650	20
B/B	+/+	38 ± 2	79 ± 3	10
B/B	0/0	72 ± 6	138 ± 10	6
C/−	+/+	85 ± 3	159 ± 5	46
C/−	+/0	104 ± 2	>300	18
C/−	0/0	144 ± 4	>300	18
D/−[c]	+/+	67	79	1

Founder mice were designated A, B, C, and D. A/−, B/−, C/−, and D/− indicate mice that are hemizygous for the transgene array. B/B indicates mice that are homozygous for the transgene array.

[a]Mean number of days ± SEM.

[b]Four of 70 offspring were transgene positive.

[c]Founder did not breed.

The conformation-dependent immunoassay was performed as described by Chiesa et al. (2003). Lysates of labeled cells prepared in buffer A were subjected to immunoprecipitation using 3F4 antibody, either with or without previous denaturation in 0.5% SDS at 95°C. The immunoprecipitated PrP was then resolved by SDS-PAGE.

Results

Spontaneous neurological illness in Tg(L9R-3AV)/*Prn-p*$^{+/+}$ mice

We introduced a murine PrP cDNA carrying the L9R-3AV mutation (Fig. 1) into the moPrP.Xho vector (Borchelt et al., 1996). This vector directs transgene expression in a pattern similar to that of endogenous PrP, with the exception that there is no expression in cerebellar Purkinje cells (Fischer et al., 1996). The mutant PrP carried an epitope for monoclonal antibody 3F4 (Bolton et al., 1991), which allowed transgenically encoded PrP to be distinguished from endogenous, murine PrP. Four founder mice (designated A–D) were obtained by pronuclear injection of fertilized oocytes from C57BL/6J × CBA/J parents (Table 1). Lines that were hemizygous for the transgene array were established from two of the founders (B and C) by breeding with nontransgenic (C57BL/6J × CBA/J) mates carrying the endogenous *Prn-p* gene.

All Tg(L9R-3AV)/*Prn-p*$^{+/+}$ mice spontaneously developed a progressive neurological illness characterized by ataxia, hindlimb paresis, and wasting (Table 1). Animals from the C line displayed an earlier onset of symptoms and shorter clinical phase before being killed than those from the B line. We intercrossed mice from the B line to produce animals homozygous for the transgene array. These animals developed symptoms shortly after weaning (38 ± 2 d), much earlier than the hemizygous B mice (172 ± 7 d), suggesting that disease onset is proportional to the expression level of mutant PrP (see below). The D founder mouse became ill at 67 d and was killed at 79 d before it could produce offspring. The A founder displayed an unusual breeding pattern. Only a small proportion (4 of 70) of transgene-positive progeny were obtained, and these were all severely runted and killed at weaning. Although this phenomenon was not investigated further, it could be attributable either to embryonic lethality of the transgene or to the presence of the transgene in only a fraction of the germ cells. In a previous study, we found that Tg(WT-E1) mice, which express wild-type PrP from the moPrP.Xho vector at levels approximately four times the endogenous PrP level, never develop clinical symptoms (Chiesa et al., 1998). Thus, the neurological illness seen in Tg(L9R-3AV) mice is related to the presence of the L9R-3AV mutation.

Neuropathology in Tg(L9R-3AV)/*Prn-p*$^{+/+}$ mice

Pathological changes were observed in the cerebellum and hippocampus of Tg(L9R-3AV)/*Prn-p*$^{+/+}$ mice from both the B and C lines. The most obvious abnormality was a marked reduction in the number of granule cells in the cerebellar cortex and a decrease in the thickness of the molecular layer (Fig. 2*A*). Loss of granule cells was most severe in the lobulus centralis, culmen, declive, uvula, and nodulus, whereas the crus II, lobulus paramedianus, and pyramis were less severely involved. Granule cells were not only fewer in number, they were also not as densely packed as normal. The molecular layer was hypercellular, and the dendrites of the Purkinje cells appeared reduced in number, although the total number of Purkinje cells appeared unchanged based on calbindin staining (data not shown). Immunohistochemical staining using anti-GFAP antibody demonstrated gliosis and astrocytic hypertrophy (Fig. 2*D*). The molecular layer displayed markedly hypertrophic Bergmann glial fibers. No spongiform changes were seen.

The hippocampus of Tg(L9R-3AV)/*Prn-p*$^{+/+}$ mice was atrophic, with reduced thickness of the pyramidal cell layer and the stratum oriens (Fig. 3*A*). The CA1 sector of the pyramidal cell layer was particularly affected. Immunohistochemical staining using anti-GFAP antibody demonstrated gliosis and astrocytic hypertrophy in the hippocampus (Fig. 3*D*).

The neurodegeneration observed in Tg(L9R-3AV)/*Prn-p*$^{+/+}$ mice was progressive, as illustrated by analysis of the cerebella of C line mice at different ages (Fig. 4). At 60 d of age, before development of symptoms, the cerebellum appeared relatively normal (Fig. 4*A*). At 85 and 99 d, after the onset of clinical symptoms, there was thinning of the granule cell and molecular layers (Fig. 4*B*,*C*). By 161 d, when animals were terminally ill, very few granule cells remained, and the cerebellum was severely atrophic (Fig. 4*D*). Our observations indicate that there is a progressive degeneration of neurons in several brain regions of Tg(L9R-3AV)/*Prn-p*$^{+/+}$ mice, although we do not rule out the possibility that there could also be effects on neuronal development and migration.

No pathological abnormalities were observed in age-matched, nontransgenic littermate mice (Figs. 2*C*,*F*, 3*C*,*F*) or in Tg(WT-E1) mice (Chiesa et al., 1998).

Neurological illness in Tg(L9R-3AV) mice is strongly dependent on coexpression of wild-type PrP

To test the effect of endogenous, wild-type PrP on the phenotype of Tg(L9R-3AV) mice, we crossed transgenic mice of the B and C lines with *Prn-p*$^{0/0}$ mice (Büeler et al., 1992) to eliminate the *Prn-p* allele. None of 20 Tg(L9R-3AV-B$^{+/-}$)/*Prn-p*$^{0/0}$ mice have shown symptoms of neurological illness, with the oldest of these living >650 d before dying of non-neurological causes (Table 1). In comparison, Tg(L9R-3AV-B$^{+/-}$)/*Prn-p*$^{+/+}$ mice first displayed symptoms at 172 d and were terminally ill by 389 d. A strong mitigating effect of eliminating the *Prn-p* allele was also evident in B line mice that were homozygous for the transgene array. Tg(L9R-3AV-B$^{+/+}$)/*Prn-p*$^{0/0}$ animals first showed symptoms at 72 d of age and became terminally ill at 138 d (Table 1). In contrast, mice homozygous for the B transgene array on the *Prn-p*$^{+/+}$ background became ill at 38 d and were terminal by 79 d. Finally, we also generated littermate Tg(L9R-3AV-C$^{+/-}$) mice on the *Prn-p*$^{+/0}$ and *Prn-p*$^{0/0}$ backgrounds. We observed that elimination of one *Prn-p* allele prolonged the onset of illness from 85 to 104 d, and elimination of both alleles delayed the onset further to 144 d. Tg(L9R-3AV-C$^{+/-}$) mice on both the *Prn-p*$^{+/0}$ and *Prn-p*$^{0/0}$ backgrounds were still alive at 300 d compared with mice on the *Prn-p*$^{+/+}$ background that were terminal by 159 d, on average. These data indicate a dose-dependent effect of endogenous PrP on the phenotype of Tg(L9R-3AV) mice.

Histological analysis confirmed the clinical results. Tg(L9R-3AV-B$^{+/-}$)/*Prn-p*$^{0/0}$ mice showed markedly improved survival of cerebellar granule cells and hippocampal pyramidal cells, as well as minimal astrogliosis, compared with age-matched Tg(L9R-3AV-B$^{+/-}$)/*Prn-p*$^{+/+}$ mice (Figs. 2*A*,*B*,*D*,*E*, 3*A*,*B*,*D*,*E*).

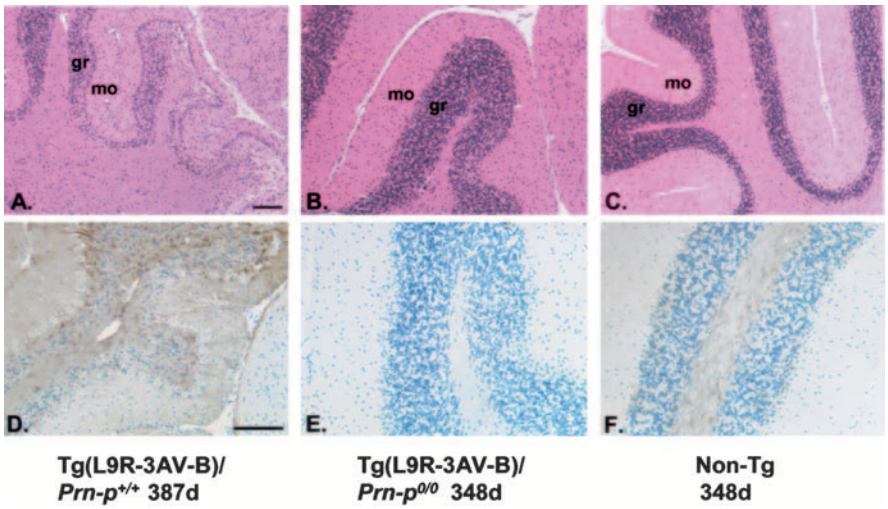

Figure 2. The histology of the cerebellum in Tg(L9R-3AV) and control mice is shown. Sections were from a Tg(L9R-3AV-B$^{+/-}$)/*Prn-p*$^{+/+}$ mouse (387 d old, symptomatic) (***A***, ***D***), a Tg(L9R-3AV-B$^{+/-}$)/*Prn-p*$^{0/0}$ mouse (348 d old, healthy) (***B***, ***E***), and a nontransgenic *Prn-p*$^{0/0}$ mouse (348 d old, healthy) (***C***, ***F***). Sections were stained with hematoxylin/eosin (***A–C***) or anti-GFAP antibody (***D–F***). gr, Granule cell layer; mo, molecular layer. Scale bars: ***A*** (for ***A–C***), ***D*** (for ***D–F***), 100 μm.

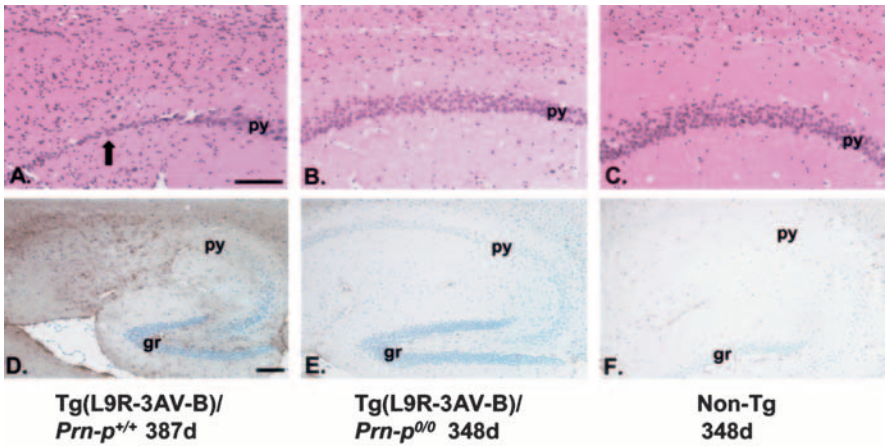

Figure 3. The histology of the hippocampus in Tg(L9R-3AV) and control mice is shown. Sections were from a Tg(L9R-3AV-B$^{+/-}$)/*Prn-p*$^{+/+}$ mouse (387 d old, symptomatic) (***A***, ***D***), a Tg(L9R-3AV-B$^{+/-}$)/*Prn-p*$^{0/0}$ mouse (348 d old, healthy) (***B***, ***E***), and a nontransgenic *Prn-p*$^{0/0}$ mouse (348 d old, healthy) (***C***, ***F***). Sections were stained with hematoxylin/eosin (***A–C***) or with anti-GFAP antibody (***D–F***). py, Pyramidal cell layer; gr, granule cell layer of the dentate gyrus. The arrow in ***A*** indicates severe loss of neurons in the pyramidal cell layer. The section shown in ***F*** was cut in a slightly different sagittal plane than those shown in ***D*** and ***E***, so the hippocampus appears larger. Scale bars: ***A*** (for ***A–C***), ***D*** (for ***D–F***), 100 μm.

Together, these results demonstrate that the neurotoxicity caused by expression of L9R-3AV PrP is dramatically accentuated by the presence of endogenous, wild-type PrP.

Transgene expression levels

Western blotting of brain homogenates from Tg(L9R-3AV) mice with 3F4 antibody revealed the presence of faint, transgene-specific PrP bands that migrated at 32–35 kDa (Fig. 5*A*, lanes 2–6). The specificity of these bands was confirmed by their absence in brain homogenates from *Prn-p*$^{0/0}$ mice (Fig. 5*A*, lane 7). The amount of L9R-3AV PrP in the runted offspring of the A founder (Fig. 5*A*, lane 2) was consistently approximately threefold higher than in mice from the B, C, or D line (Fig. 5*A*, lanes 3–5), confirming that the onset of the neurological illness in Tg(L9R-3AV) mice is correlated with the expression level of mutant PrP. However, the levels of L9R-3AV PrP observed by Western blotting in all transgenic lines were extremely low, ~1–5% of the level of endogenous PrP (data not shown) or of transgenically encoded PrP in Tg(WT-E1) mice (Fig. 5*A*, lane 1). This fact made it difficult to reliably compare the relative expression levels of the B, C, and D lines. However, our impression is that the C line expresses slightly more PrP than the B line, thus accounting for the earlier disease onset seen in the former line (Table 1).

Two kinds of experiments indicated that Western blotting significantly underestimated the amount of L9R-3AV PrP. First, reverse transcriptase (RT)-PCR was performed to estimate the levels of both transgene-derived and endogenous PrP mRNA in the brain using primer pairs specific to each species (Fig. 5*B*). Because the two PrP mRNAs were amplified in separate reactions, β-actin mRNA was used as an internal standard for RNA input to allow comparison of the PrP mRNA signals from the two reactions. The ratios of transgenic:endogenous PrP mRNA were 2.9, 1.3, and 1.4 for mice from the A, B, and C lines, respectively

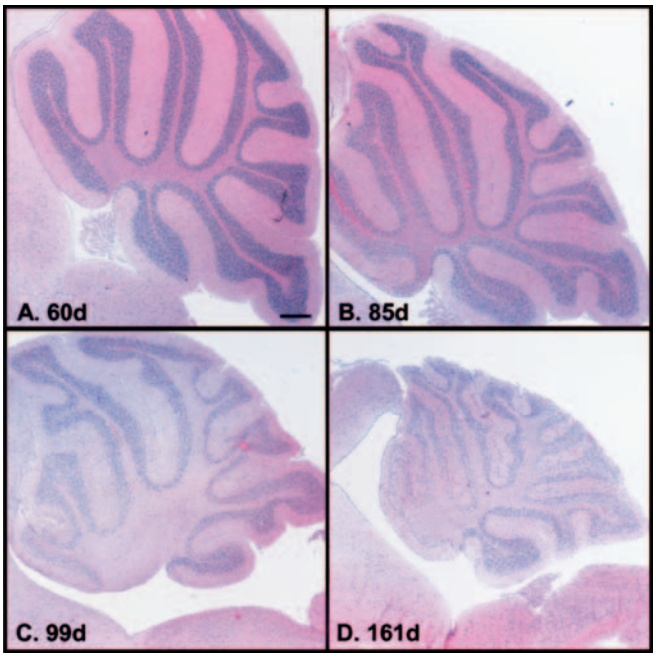

Figure 4. Neurodegeneration in the cerebellum of Tg(L9R-3AV) is progressive. Sections from Tg(L9R-3AV-C $^{+/-}$)/*Prn-p* $^{+/+}$ mice of the indicated ages were stained with hematoxylin/eosin. The 60-d-old mouse (***A***) was healthy, the 85- and 99-d-old mice (***B*** and ***C***, respectively) were symptomatic, and the 161-d-old mouse (***D***) was terminal. Scale bar: (in ***A***) ***A–D***, 100 μm.

(Fig. 5*B*, lanes 2–4). In comparison, Tg(PG14) and Tg(WT) mice (Chiesa et al., 1998) showed ratios of 1.0 and 3.6, respectively, consistent with their previously determined PrP protein expression levels of 1× and 3.6× endogenous (Fig. 5*B*, lanes 7, 8). As expected, nontransgenic *Prn-p* $^{+/+}$ mice showed only a band corresponding to endogenous PrP mRNA (Fig. 5*B*, lane 1), and nontransgenic *Prn-p* $^{0/0}$ mice showed no PrP mRNA bands (Fig. 5*B*, lane 5). Thus, we estimate that transgene mRNA is expressed in the brain at levels well above those that would be predicted based on Western blotting for PrP protein.

In a second experiment, we compared PrP protein levels in CGNs cultured from Tg(L9R-3AV-B $^{+/-}$)/*Prn-p* $^{0/0}$ and Tg(WT) mice using either immunoprecipitation or Western blotting. Immunoprecipitation of PrP from [^{35}S]methionine-labeled cells using either the 8H4 or 3F4 antibody revealed that the amount of PrP in Tg(L9R-3AV) neurons was 30% of the amount in Tg(WT) neurons (Fig. 5*C*, IP). Because the endogenous PrP level in nontransgenic mice is ~30% of the level of transgenic PrP in Tg(WT) mice (Chiesa et al., 1998), the immunoprecipitation results imply that Tg(L9R-3AV-B $^{+/-}$) mice express mutant PrP at approximately endogenous levels. In contrast, when samples from parallel cultures were subjected to Western blotting using the 8H4 or 3F4 antibody (Fig. 5*C*, WB), the amount of L9R-3AV PrP detected was only 1–5% of the amount of wild-type PrP. This discrepancy between the immunoprecipitation and Western blot results does not result from rapid metabolic turnover of L9R-3AV PrP, which has a half-life in neurons similar to that of the wild-type protein (Stewart and Harris, 2005). Rather, our results indicate that L9R-3AV PrP reacts poorly on Western blots, although it is detected efficiently by immunoprecipitation after SDS denaturation. The explanation for the poor reactivity of the mutant PrP on Western blots is unknown but may be related to masking of antibody epitopes in the protein when it is bound to the Nylon membrane either as a result of the mutations or the presence of the hydrophobic signal peptide (Stewart and Harris, 2005).

Using both Western blotting (Fig. 5*A*, lanes 3, 6) and RT-PCR (Fig. 5*B*, lanes 3, 6), we have confirmed that transgene expression levels are similar in Tg(L9R-3AV) mice on the *Prn-p* $^{0/0}$ and *Prn-p* $^{+/+}$ backgrounds. Thus, a reduction in expression of mutant PrP cannot account for the ameliorated phenotype of Tg(L9R-3AV)/*Prn-p* $^{0/0}$ mice.

Tg(L9R-3AV) neurons produce both ^{Ctm}PrP and ^{Sec}PrP

To assay the membrane topology of PrP in neurons from Tg(L9R-3AV) mice, we used primary cultures of cerebellar granule cells, which comprise one of the neuronal populations that degenerate *in vivo* in these animals. Dissociated neurons were labeled with [^{35}S]methionine, and then microsomes present in a postnuclear supernatant were subjected to protease digestion, followed by immunoprecipitation of PrP using 3F4 antibody. In this assay, fully translocated PrP (^{Sec}PrP) is completely protected from digestion, yielding a 25–27 kDa band after enzymatic deglycosylation. ^{Ctm}PrP produces a 19 kDa protected fragment, representing the lumenal and transmembrane domains of the protein. We found that microsomes from Tg(L9R-3AV-B $^{+/-}$)/*Prn-p* $^{+/+}$ neurons yielded approximately equal amounts of the 27 and 19 kDa bands, implying that these cells contained equal proportions of ^{Sec}PrP and ^{Ctm}PrP (Fig. 6, lane 5). We did not detect a 15 kDa fragment indicative of ^{Ntm}PrP. Protease treatment of microsomes in the presence of detergent eliminated both the 19 and 27 kDa bands (Fig. 6, lane 6), confirming that these species arose from protection by the microsomal membrane, rather than from intrinsic protease resistance of PrP. Identical results were obtained with neurons cultured from Tg(L9R-3AV-B $^{+/-}$)/*Prn-p* $^{0/0}$ and Tg(L9R-3AV-C $^{+/-}$)/*Prn-p* $^{+/+}$ mice (data not shown). As expected, microsomes from Tg(WT) neurons showed only a fully protected band of 25 kDa corresponding to ^{Sec}PrP (Fig. 6, lane 2). We confirmed, as reported previously (Stewart et al., 2001), that L9R-3AV PrP expressed in transfected Chinese hamster ovary (CHO) cells produces only a single, protease-protected band of 19 kDa (Fig. 6, lane 8). Thus, CHO cells synthesize the mutant protein exclusively with the ^{Ctm}PrP topology, without detectable ^{Sec}PrP. These results indicate that the L9R-3AV mutation significantly increases the ratio of ^{Ctm}PrP to ^{Sec}PrP in CGNs as well as in CHO cells, but the effect is less pronounced in the neurons.

^{Sec}PrP is localized to the cell surface, and ^{Ctm}PrP is localized to the Golgi apparatus

We used immunofluorescence staining in conjunction with phospholipase treatment to determine the subcellular distribution of ^{Ctm}PrP and ^{Sec}PrP in neurons from Tg(L9R-3AV) mice. PIPLC is a bacterial enzyme that cleaves the GPI anchor at the C terminus of PrP. PIPLC treatment is predicted to release ^{Sec}PrP but not ^{Ctm}PrP from cell membranes, because the latter form has a transmembrane anchor in addition to a GPI anchor. When we stained living (nonpermeabilized) neurons from Tg(L9R-3AV-B $^{+/-}$)/*Prn-p* $^{0/0}$ mice with any of several anti-PrP antibodies, we found that the mutant protein was distributed along the surface of neuronal processes that formed a dense meshwork in the culture (Fig. 7*A*). When cultures were treated with PIPLC, virtually all of the PrP was released from the neuronal surface (Fig. 7*B*). This result implies that most of the surface PrP has the ^{Sec}PrP topology. Identical results were obtained with neurons from Tg(L9R-3AV-B $^{+/-}$)/*Prn-p* $^{+/+}$ mice (data not shown).

Because little ^{Ctm}PrP was present on the surface, most of this form must be localized to intracellular compartments. We

stained Triton X-100-permeabilized neurons to visualize intracellular PrP. We observed that the mutant protein was present in discrete, perinuclear structures in the soma that colocalized with the Golgi marker protein giantin (Fig. 7*C–E*). Surface staining was less prominent in these permeabilized neurons, because Triton X-100 partially extracts PrP from the plasma membrane and also enhances the reactivity of cytoplasmic epitopes of Golgi-resident PrP (our unpublished observations). The distribution of PrP was identical in neurons from Tg(L9R-3AV)/*Prn-p*$^{+/+}$ and Tg(L9R-3AV)/*Prn-p*$^{0/0}$ mice from both the B and C lines (data not shown). Using immunofluorescence staining in conjunction with methods for differential permeabilization of the plasma membrane and intracellular membranes, we have demonstrated directly that PrP in the Golgi of Tg(L9R-3AV) neurons has the ^{Ctm}PrP topology (Stewart and Harris, 2005). In control experiments (data not shown), we found that wild-type PrP in neurons from nontransgenic mice was distributed primarily along the surface of neuronal processes, with little detectable intracellular staining. Thus, the ^{Ctm}PrP form of L9R-3AV PrP is concentrated in the Golgi apparatus of neurons, whereas the ^{Sec}PrP form is present on the surface of neuronal processes.

To confirm that the results obtained in cultured neurons were also applicable to brain tissue, we performed immunohistochemical staining of PrP in Triton X-100-permeabilized brain sections from Tg(L9R-3AV) mice. In the granule cell layer of the cerebellum, we found that L9R-3AV PrP was concentrated in small foci within granule cell bodies that colocalized with giantin (Fig. 7*F–H*), similar to the distribution of the protein in cultured neurons. In contrast, sections from nontransgenic control mice showed strong staining for wild-type PrP in the glomeruli surrounding granule neurons but little staining within the granule cell bodies themselves (Fig. 7*I–K*). Staining of Triton X-100-treated sections from the cerebral cortex and hippocampus of Tg(L9R-3AV) mice also revealed Golgi-localized PrP in the cell bodies of many neurons (data not shown).

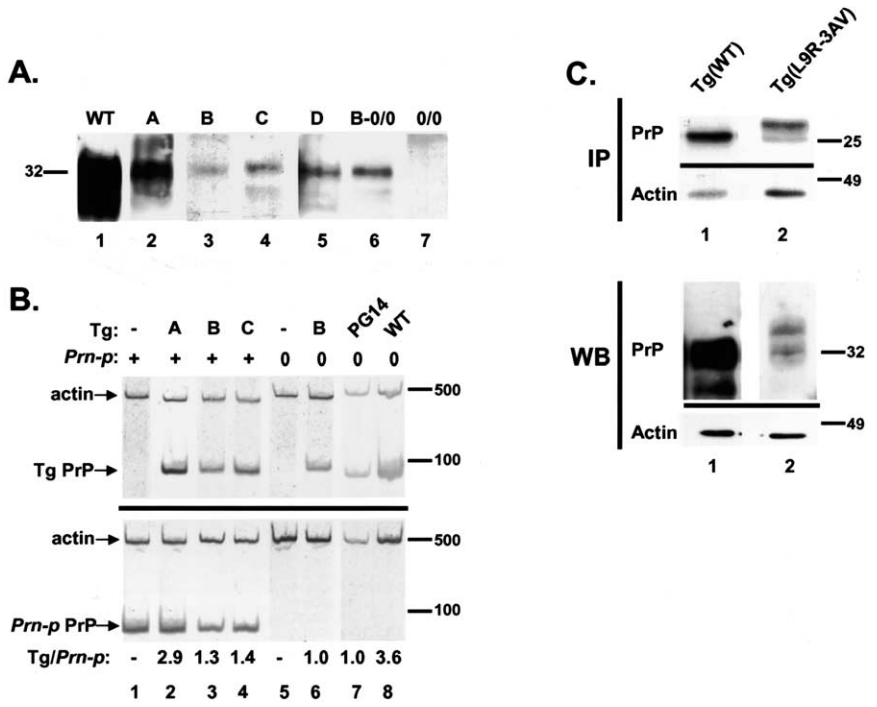

Figure 5. Expression of PrP in the brain and in cultured neurons from Tg(L9R-3AV) mice. ***A***, Brain homogenates from the following mice were analyzed by Western blotting using anti-PrP antibody 3F4: lane 1, Tg(WT); lanes 2–5, Tg(L9R-3AV $^{+/-}$)/*Prn-p*$^{+/+}$ lines A–D, respectively; lane 6, Tg(L9R-3AV $^{+/-}$)/*Prn-p*$^{0/0}$ line B; lane 7, nontransgenic *Prn-p*$^{0/0}$. Lane 1 was exposed for a shorter time than the other lanes. The molecular size marker is in kilodaltons. ***B***, RNA was extracted from the brains of mice whose transgene (Tg) and *Prn-p* status are indicated above each lane. For transgene status, A, B, and C indicate lines of Tg(L9R-3AV $^{+/-}$) mice, and a − symbol indicates that the mouse is nontransgenic. For *Prn-p* status, the + symbol indicates *Prn-p*$^{+/+}$, and the 0 symbol indicates *Prn-p*$^{0/0}$. RT-PCR was performed using primers specific for mouse β-actin and transgenically encoded PrP (top) or for mouse β-actin and endogenous (*Prn-p*-encoded) PrP (bottom). PCR products (indicated by arrows) were resolved by PAGE and stained with SYBRGreen. Tg/*Prn-p* indicates the calculated ratio of transgenically encoded to endogenous PrP. Size markers are given in nucleotides. ***C***, Duplicate cultures of cerebellar granule cells were prepared from Tg(WT) mice (lane 1) or from Tg(L9R-3AV-B $^{+/-}$)/*Prn-p*$^{0/0}$ mice (lane 2). One culture of each pair was labeled for 4 h with [^{35}S]methionine, and then PrP and actin were detected by immunoprecipitation (IP) followed by SDS-PAGE and autoradiography. The other culture of the pair was lysed, and PrP and actin were visualized by Western blotting (WB). 8H4 antibody was used to detect PrP in the experiments shown here, but similar results were obtained with 3F4 antibody (data not shown). Proteins were enzymatically deglycosylated before immunoprecipitation. In the IP experiment, the slightly slower migration of L9R-3AV PrP compared with wild-type PrP is attributable to the presence of the signal peptide on the mutant protein (Stewart and Harris, 2005).

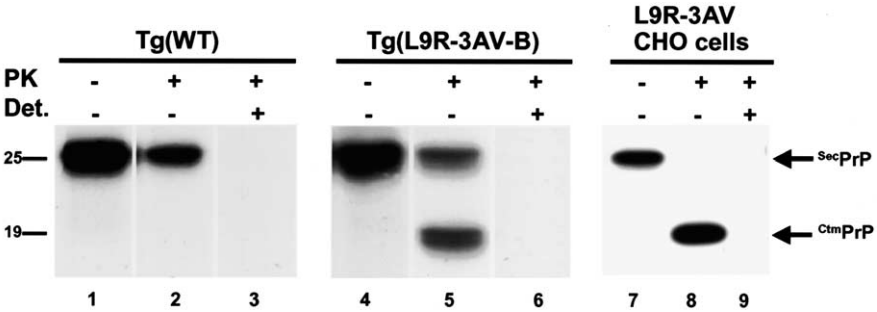

Figure 6. Neurons from Tg(L9R-3AV) mice produce both ^{Ctm}PrP and ^{Sec}PrP. CGNs cultured from Tg(WT) (lanes 1–3) or Tg(L9R-3AV-B $^{+/-}$)/*Prn-p*$^{+/+}$ (lanes 4–6) mice were labeled for 4 h with [^{35}S]methionine. CHO cells were transiently transfected with a plasmid encoding L9R-3AV PrP (lanes 7–9). Postnuclear supernatants from all cultures were then incubated with (lanes 2, 3, 5, 6, 8, 9) or without (lanes 1, 4, 7) PK in the presence (lanes 3, 6, 9) or absence (lanes 1, 2, 4, 5, 7, 8) of Triton X-100 (Det.). Proteins were then solubilized in SDS and enzymatically deglycosylated, and PrP was detected either by immunoprecipitation with 3F4 antibody (lanes 1–6) or by Western blotting with 3F4 antibody (lanes 7–9). The protease-protected forms of ^{Sec}PrP and ^{Ctm}PrP are indicated by arrows to the right of the gels.

L9R-3AV PrP does not have PrP^{Sc} properties

Previous studies have shown that ^{Ctm}PrP can cause neurodegeneration in the absence of PrP^{Sc} (Hegde et al., 1998b, 1999). We therefore tested whether PrP from Tg(L9R-3AV) mice displayed three characteristic biochemical properties of PrP^{Sc}: detergent insolubility, protease resistance, and a conformational alteration that alters antibody accessibility. As a control, we analyzed PrP from Tg(WT) and Tg(PG14) mice. Tg(PG14) mice express an insertionally mutated PrP that exhibits several PrP^{Sc}-like features (Chiesa et al., 1998). We performed these ex-

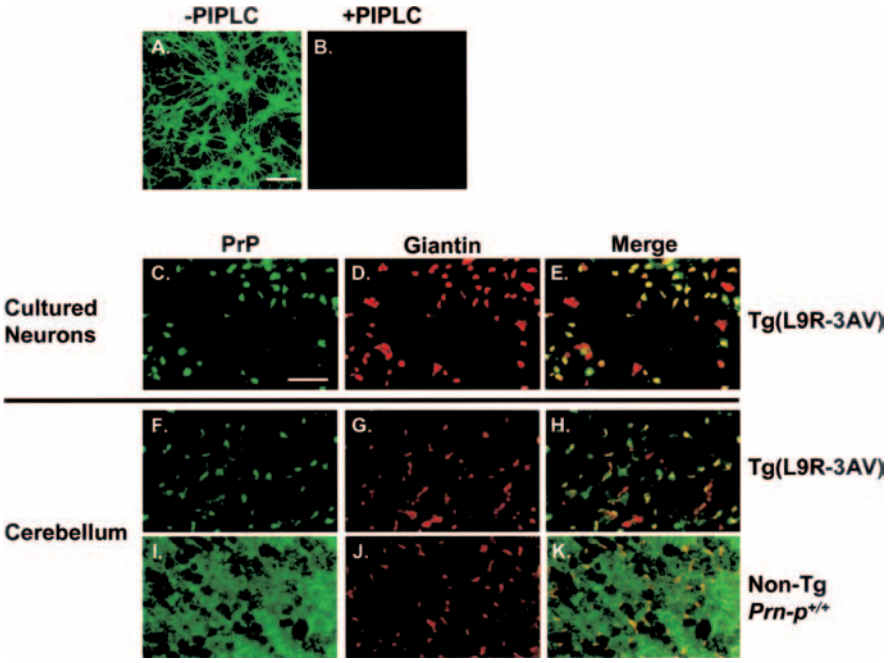

Figure 7. ^{Sec}PrP is localized to the cell surface, and ^{Ctm}PrP is localized to the Golgi apparatus. ***A***, ***B***, Cerebellar granule cells cultured from Tg(L9R-3AV-B $^{+/-}$)/*Prn-p*$^{0/0}$ mice were incubated with (***B***) or without (***A***) PIPLC and stained without permeabilization using 8H4 antibody to reveal surface PrP. ***C–E***, Cerebellar granule cells cultured from Tg(L9R-3AV-B $^{+/-}$)/*Prn-p*$^{0/0}$ mice were fixed, permeabilized with Triton X-100, and stained with anti-PrP (8B4) and anti-giantin antibodies. A green-labeled secondary antibody was used to visualize PrP (***C***), and a red-labeled secondary antibody was used to visualize giantin (***D***). ***E***, Merged image of the green and red channels demonstrating colocalization of PrP and giantin (yellow). A few cells show only red staining for giantin, presumably because they express lower levels of PrP. ***F–K***, Permeabilized vibratome sections from the cerebella of Tg(L9R-3AV-B $^{+/+}$)/*Prn-p*$^{0/0}$ (***F–H***) or nontransgenic (Non-Tg) *Prn-p*$^{+/+}$ (***I–K***) mice were stained with anti-PrP (8B4) and anti-giantin antibodies. A green-labeled secondary antibody was used to visualize PrP (***F***, ***I***) and a red-labeled secondary antibody was used to visualize giantin (***G***, ***J***). ***H***, ***K***, Merged images of the green and red channels. Images are taken from the granule cell layer of the cerebellum. Scale bars: ***A*** (for ***A***, ***B***), ***C*** (for ***C–K***), 25 μm.

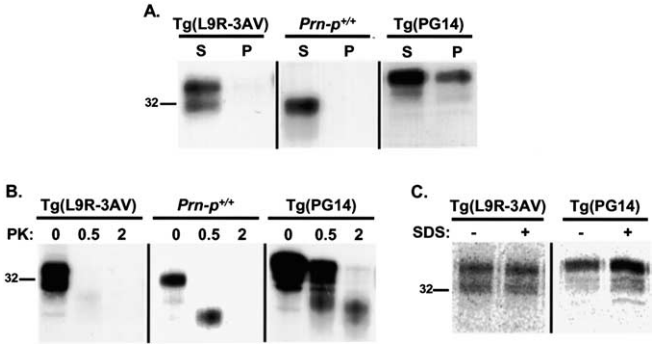

Figure 8. L9R-3AV PrP does not have PrP^{Sc} properties. ***A***, Cerebellar granule cells cultured from Tg(L9R-3AV-B $^{+/-}$)/*Prn-p*$^{+/+}$, nontransgenic *Prn-p*$^{+/+}$, or Tg(PG14) mice were labeled with [^{35}S]methionine for 4 h, and cell lysates were centrifuged at 10,000 $\times$ *g* for 10 min. The supernatant was recentrifuged at 180,000 $\times$ *g* for 45 min, and PrP in supernatant (S) and pellet (P) fractions was immunoprecipitated with 3F4 antibody [Tg(L9R-3AV), Tg(PG14)] or 8H4 antibody (*Prn-p*$^{+/+}$). ***B***, Granule cells were labeled as in ***A***. Clarified cell lysates were incubated with the indicated amounts of PK (in micrograms per milliliter) at 37°C for 20 min, after which PrP was immunoprecipitated with 3F4 antibody [Tg(L9R-3AV), Tg(PG14)] or 8H4 antibody (*Prn-p*$^{+/+}$). ***C***, Granule cells were labeled as in ***A***. PrP was immunoprecipitated from cell lysates with 3F4 antibody, either with (+) or without (−) previous denaturation in the presence of SDS.

periments by labeling cultured cerebellar neurons with [^{35}S]methionine and collecting PrP by immunoprecipitation.

In the assay for detergent insolubility (Fig. 8*A*), we found that mutant PrP in Tg(L9R-3AV) mice, like wild-type PrP in nontransgenic *Prn-p*$^{+/+}$ mice, remained in the supernatant after ultracentrifugation of a detergent lysate. In contrast, a portion of PG14 PrP was found in the pellet fraction. In the protease-resistance assay (Fig. 8*B*), we observed that L9R-3AV PrP and wild-type PrP were sensitive to digestion with low concentrations of PK under conditions in which PG14 PrP yielded a characteristic, protease-resistant fragment of 27–30 kDa. We also performed a conformation-dependent immunoassay to test the accessibility of the 3F4 epitope of PrP under native and denatured conditions (Fig. 8*C*). PrP^{Sc} and PG14 PrP, but not wild-type PrP^{C}, display a buried 3F4 epitope under native conditions (Safar et al., 1998; Chiesa et al., 2003). We found that L9R-3AV PrP (as well as wild-type PrP; data not shown) could be immunoprecipitated with 3F4 equally well in the native state and after SDS denaturation. In contrast, PG14 PrP reacted more efficiently with 3F4 after denaturation. These results indicate that L9R-3AV PrP in neurons does not display any of three biochemical signatures of PrP^{Sc}.

We also failed to detect detergent-insoluble or protease-resistant PrP when we analyzed brain homogenates from symptomatic Tg(L9R-3AV)/*Prn-p*$^{+/+}$ mice by Western blotting using either 3F4 or 8H4 antibody (data not shown). These results indicate that neither L9R-3AV PrP nor endogenous PrP is converted to a PrP^{Sc} state in clinically ill mice. We also inoculated brain homogenates from ill Tg(L9R-3AV)/*Prn-p*$^{+/+}$ mice of the B and C lines into Tga20 $^{+/0}$ indicator mice (Fischer et al., 1996) to assay for infectivity. The inoculated animals have remained healthy for >270 d, whereas Tga20 $^{+/0}$ mice inoculated with Rocky Mountain Laboratory prions become ill after 92 ± 4 d (our unpublished data). Thus, L9R-3AV PrP does not generate infectious prions.

Discussion

We have produced a neurological disorder in transgenic mice by expression of a PrP molecule that carries mutations (L9R-3AV) favoring synthesis of ^{Ctm}PrP, a transmembrane form of PrP. These mice develop severe ataxia accompanied by dramatic loss of cerebellar granule cells and hippocampal pyramidal cells. Unexpectedly, we found that development of this phenotype is strongly dependent on coexpression of endogenous, wild-type PrP. Our results provide new insights into several key issues, including the neuronal cell biology of ^{Ctm}PrP, the mechanisms of PrP-related neurotoxicity, and possible cellular activities of PrP^{C}.

Comparison of Tg(L9R-3AV) mice with other transgenic models

Hegde et al. (1998b, 1999) have previously described transgenic mice that express PrP molecules carrying mutations in the central region alone, including 3AV, that favor synthesis of ^{Ctm}PrP. These mice spontaneously develop a neurodegenerative illness characterized by ataxia and astrocytic gliosis, but without PrP^{Sc}. The mice created by Hegde et al. (1998b, 1999) differ from our Tg(L9R-3AV) mice in several important respects. First, they synthesize lower proportions of ^{Ctm}PrP (20–30%, depending on the

mutation, compared with 50% for L9R-3AV). This difference reflects the fact that mutations in the signal sequence such as L9R enhance production of ^{Ctm}PrP (Stewart and Harris, 2003). Second, the mice in the study by Hegde et al. (1998b, 1999) developed illness at much later times than our Tg(L9R-3AV) mice, when one compares lines that have an equivalent "^{Ctm}PrP index" [% ^{Ctm}PrP × Tg expression level, as defined by Hegde et al. (1999)]. We suggest that this discrepancy reflects the fact that the mice in the study by Hegde et al. (1998b, 1999) were created on the *Prn-p*$^{0/0}$ background and that introduction of the wild-type PrP allele would significantly shorten the incubation time in these animals. We hypothesize that because the mice in the study by Hegde et al. (1998b, 1999) converted proportionally more of their mutant PrP to the ^{Sec}PrP form than Tg(L9R-3AV) mice, this may be sufficient to allow disease development in the absence of endogenous, wild-type ^{Sec}PrP (see below).

Differences between transgenic neurons and transfected cells in ^{Ctm}PrP synthesis and localization

We demonstrated previously that L9R-3AV PrP is synthesized almost exclusively with the ^{Ctm}PrP topology in transiently transfected CHO, baby hamster kidney (BHK), and N2a cells (Stewart et al., 2001; Stewart and Harris, 2003). In contrast, we found that CGNs from Tg(L9R-3AV) mice express ~50% of the mutant protein as ^{Ctm}PrP and ~50% as ^{Sec}PrP. The reasons for this difference between transfected cells and granule neurons remain to be determined. One plausible explanation is that granule neurons and transformed cell lines differ in their content of protein factors that have been shown to influence the membrane topology of PrP during ER translocation (Hegde et al., 1998a; Fons et al., 2003). It is also possible that neurons possess mechanisms for selectively degrading ^{Ctm}PrP.

There is also a difference between granule neurons and transfected cells in the localization of ^{Ctm}PrP. Although most of the ^{Ctm}PrP in granule neurons from Tg(L9R-3AV) mice resides in the Golgi apparatus (this work; Stewart and Harris, 2005), most of the ^{Ctm}PrP in transfected CHO, BHK, and N2a cells expressing L9R-3AV PrP is localized to the ER (Stewart et al., 2001). We have observed that L9R-3AV PrP in fibroblasts cultured from Tg(L9R-3AV) mice is endoglycosidase H resistant (our unpublished data), arguing that the protein is trafficked to a post-ER compartment in these cells as well. Thus, factors other than cell type are likely to determine the localization of the mutant protein. It is possible that the high expression levels characteristic of transiently transfected cells cause ER retention of ^{Ctm}PrP, whereas the more physiological levels present in cells from transgenic mice allows the protein to transit further along the secretory pathway.

What is the neurotoxic species in Tg(L9R-3AV) mice, and what is its locus of action?

Tg(L9R-3AV) mice produce approximately equal proportions of mutant ^{Ctm}PrP and ^{Sec}PrP, raising the question of which of these species is responsible for the neurodegeneration seen in these animals. Two considerations argue against ^{Sec}PrP being the neurotoxic species. First, ^{Sec}PrP produced in Tg(L9R-3AV) mice behaves like wild-type PrP^{C} in terms of its cellular trafficking and biochemical properties. Second, mutations other than L9R-3AV that favor synthesis of ^{Ctm}PrP also cause neurodegeneration when expressed in transgenic mice (Hegde et al., 1998b, 1999). Thus, the L9R-3AV mutation is likely to be neurotoxic because of its effect on ^{Ctm}PrP production, rather than because of a specific alteration of the PrP amino acid sequence. It is unlikely that the neurological illness in Tg(L9R-3AV) mice is related to generation of PrP^{Sc}, because PrP from these animals does not display any of the characteristic biochemical properties of PrP^{Sc}, and the brains of these animals do not contain prion infectivity.

The localization of ^{Ctm}PrP in the Golgi apparatus raises the possibility that the neurotoxic effects of ^{Ctm}PrP may involve this organelle. The Golgi apparatus undergoes a dramatic disassembly process during apoptosis (Maag et al., 2003; Machamer, 2003). In addition, there are several caspase substrates, and at least one procaspase and a caspase inhibitor, that reside in this organelle. Thus, it is possible that ^{Ctm}PrP in the Golgi directly initiates apoptotic signals or amplifies signals that originate elsewhere in the cell.

Why is neurodegeneration in Tg(L9R-3AV) mice dependent on expression of endogenous PrP?

The most intriguing and unexpected observation to emerge from our studies is that the phenotype of Tg(L9R-3AV) mice is greatly accentuated by coexpression of endogenous, wild-type PrP. The effect of endogenous PrP is dose dependent, because Tg(L9R-3AV) mice on the *Prn-p*$^{+/0}$ background display a disease onset intermediate between that of mice on the *Prn-p*$^{0/0}$ and *Prn-p*$^{+/+}$ backgrounds. This latter result makes it unlikely that the amelioration of the phenotype associated with elimination of *Prn-p* alleles is attributable to segregation of unrelated background genes. We have ruled out several other explanations for the phenotypic disparity between mice on the *Prn-p*$^{0/0}$ and *Prn-p*$^{+/+}$ backgrounds, including differences in transgene expression level and alterations in the transgene sequence. In addition, we have confirmed that the proportion of ^{Ctm}PrP and the subcellular localization of this form are similar in CGNs of mice from both backgrounds.

Our results suggest that expression of ^{Ctm}PrP causes neurodegeneration via a process in which endogenous, wild-type PrP^{C} participates. How might this occur? Two possible models are shown in supplemental Figure 1 (available at www.jneurosci.org as supplemental material). In the simplest scheme (supplemental Fig. 1*A*, available at www.jneurosci.org as supplemental material), ^{Ctm}PrP binds to wild-type PrP^{C} (presumably in the ^{Sec}PrP form), resulting in generation of a neurotoxic signal. We also envision a second, more complex model (supplemental Fig. 1*B*, available at www.jneurosci.org as supplemental material) that takes into account a purported physiological function of PrP^{C}, namely its ability to protect neurons from various toxic insults (for review, see Roucou et al., 2004). In this scheme, PrP^{C} normally interacts with another molecule, Tr, that serves a transducer of a neuroprotective signal [supplemental Fig. 1*B* (left), available at www.jneurosci.org as supplemental material]. Because *Prn-p*$^{0/0}$ mice are phenotypically normal (Büeler et al., 1992), this neuroprotective signal would have to be nonessential under most conditions. When ^{Ctm}PrP is present along with ^{Sec}PrP, both proteins bind to Tr, causing the latter to undergo a conformational change to the Tr* state, which delivers a neurotoxic rather than a neuroprotective signal [supplemental Fig. 1*B* (right), available at www.jneurosci.org as supplemental material]. In this model, ^{Ctm}PrP is neurotoxic because it causes an inversion of the normal, neuroprotective activity of PrP^{C}. In both models, the ^{Sec}PrP component could be supplied either by endogenous, wild-type PrP or less efficiently by transgenically encoded L9R-3AV PrP if it were present in sufficient amounts. This hypothesis would explain why deleting the *Prn-p* gene ameliorated but did not completely prevent development of neurological symptoms in Tg(L9R-3AV-C$^{+/-}$)/*Prn-p*$^{0/0}$ and Tg(L9R-3AV-B$^{+/+}$)/*Prn-p*$^{0/0}$ mice. In these animals, the amount of

mutant ^{Sec}PrP may be sufficient to transmit the neurotoxic signal in the absence of endogenous ^{Sec}PrP. The fact that ^{Ctm}PrP is concentrated in the Golgi apparatus of neurons, whereas ^{Sec}PrP is found primarily on the cell surface, does not mitigate against a physical interaction of the two proteins, because ^{Sec}PrP must transit the Golgi on its way to the cell surface.

A new view of the role of ^{Ctm}PrP in prion biology

In this study, we demonstrate that ^{Ctm}PrP-associated neurodegeneration is highly dependent on the presence of wild-type PrP^{C}. This observation potentially connects the toxic activity of ^{Ctm}PrP to the normal, physiological function of PrP^{C}. There are several other situations in which expression of PrP^{C} in target neurons appears to be essential for conferring sensitivity to PrP-related neurotoxic insults (Brown et al., 1994; Brandner et al., 1996; Mallucci et al., 2003; Solforosi et al., 2004). Each of these situations could conceivably reflect the operation of a neurotoxic, PrP^{C}-dependent signaling pathway similar to the one we postulate is activated by ^{Ctm}PrP. Interestingly, the ability of PrP^{C} to accentuate the phenotype of Tg(L9R-3AV) mice appears to be the inverse of its ability to rescue the neurodegenerative phenotype of transgenic mice that ectopically express Doppel (Moore et al., 2001; Rossi et al., 2001) and N-terminally truncated PrP (Shmerling et al., 1998). It will be of great interest to determine whether these two contrasting activities of PrP^{C} are related and, if so, what molecular mechanisms account for whether PrP^{C} delivers a neurotoxic or neuroprotective signal.

References

Bolton DC, Seligman SJ, Bablanian G, Windsor D, Scala LJ, Kim KS, Chen CM, Kascsak RJ, Bendheim PE (1991) Molecular location of a species-specific epitope on the hamster scrapie agent protein. J Virol 65:3667–3675.

Borchelt DR, Davis J, Fischer M, Lee MK, Slunt HH, Ratovitsky T, Regard J, Copeland NG, Jenkins NA, Sisodia SS, Price DL (1996) A vector for expressing foreign genes in the brains and hearts of transgenic mice. Genet Anal Biomol Eng 13:159–163.

Brandner S, Isenmann S, Raeber A, Fischer M, Sailer A, Kobayashi Y, Marino S, Weissmann C, Aguzzi A (1996) Normal host prion protein necessary for scrapie-induced neurotoxicity. Nature 379:339–343.

Brown DR, Herms J, Kretzschmar HA (1994) Mouse cortical cells lacking cellular PrP survive in culture with a neurotoxic PrP fragment. NeuroReport 5:2057–2060.

Büeler H, Fischer M, Lang Y, Fluethmann H, Lipp H-P, DeArmond SJ, Prusiner SB, Aguet M, Weissmann C (1992) Normal development and behavior of mice lacking the neuronal cell-surface PrP protein. Nature 356:577–582.

Chiesa R, Harris DA (2001) Prion diseases: what is the neurotoxic molecule? Neurobiol Dis 8:743–763.

Chiesa R, Piccardo P, Ghetti B, Harris DA (1998) Neurological illness in transgenic mice expressing a prion protein with an insertional mutation. Neuron 21:1339–1351.

Chiesa R, Piccardo P, Quaglio E, Drisaldi B, Si-Hoe SL, Takao M, Ghetti B, Harris DA (2003) Molecular distinction between pathogenic and infectious properties of the prion protein. J Virol 77:7611–7622.

Drisaldi B, Stewart RS, Adles C, Stewart LR, Quaglio E, Biasini E, Fioriti L, Chiesa R, Harris DA (2003) Mutant PrP is delayed in its exit from the endoplasmic reticulum, but neither wild-type nor mutant PrP undergoes retrotranslocation prior to proteasomal degradation. J Biol Chem 278:21732–21743.

Fischer M, Rülicke T, Raeber A, Sailer A, Moser M, Oesch B, Brandner S, Aguzzi A, Weissmann C (1996) Prion protein (PrP) with amino-proximal deletions restoring susceptibility of PrP knockout mice to scrapie. EMBO J 15:1255–1264.

Fons RD, Bogert BA, Hegde RS (2003) Substrate-specific function of the translocon-associated protein complex during translocation across the ER membrane. J Cell Biol 160:529–539.

Hegde RS, Voigt S, Lingappa VR (1998a) Regulation of protein topology by *trans*-acting factors at the endoplasmic reticulum. Mol Cell 2:85–91.

Hegde RS, Mastrianni JA, Scott MR, Defea KA, Tremblay P, Torchia M, DeArmond SJ, Prusiner SB, Lingappa VR (1998b) A transmembrane form of the prion protein in neurodegenerative disease. Science 279:827–834.

Hegde RS, Tremblay P, Groth D, DeArmond SJ, Prusiner SB, Lingappa VR (1999) Transmissible and genetic prion diseases share a common pathway of neurodegeneration. Nature 402:822–826.

Hölscher C, Bach UC, Dobberstein B (2001) Prion protein contains a second endoplasmic reticulum targeting signal sequence located at its C terminus. J Biol Chem 276:13388–13394.

Kim SJ, Rahbar R, Hegde RS (2001) Combinatorial control of prion protein biogenesis by the signal sequence and transmembrane domain. J Biol Chem 276:26132–26140.

Maag RS, Hicks SW, Machamer CE (2003) Death from within: apoptosis and the secretory pathway. Curr Opin Cell Biol 15:456–461.

Machamer CE (2003) Golgi disassembly in apoptosis: cause or effect? Trends Cell Biol 13:279–281.

Mallucci G, Dickinson A, Linehan J, Klohn PC, Brandner S, Collinge J (2003) Depleting neuronal PrP in prion infection prevents disease and reverses spongiosis. Science 302:871–874.

Miller TM, Johnson Jr EM (1996) Metabolic and genetic analyses of apoptosis in potassium/serum-deprived rat cerebellar granule cells. J Neurosci 16:7487–7495.

Moore RC, Mastrangelo P, Bouzamondo E, Heinrich C, Legname G, Prusiner SB, Hood L, Westaway D, DeArmond SJ, Tremblay P (2001) Doppel-induced cerebellar degeneration in transgenic mice. Proc Natl Acad Sci USA 98:15288–15293.

Prusiner SB (1998) Prions. Proc Natl Acad Sci USA 95:13363–13383.

Rossi D, Cozzio A, Flechsig E, Klein MA, Rulicke T, Aguzzi A, Weissmann C (2001) Onset of ataxia and Purkinje cell loss in PrP null mice inversely correlated with Dpl level in brain. EMBO J 20:694–702.

Roucou X, Gains M, LeBlanc AC (2004) Neuroprotective functions of prion protein. J Neurosci Res 75:153–161.

Safar J, Wille H, Itrri V, Groth D, Serban H, Torchia M, Cohen FE, Prusiner SB (1998) Eight prion strains have PrP^{Sc} molecules with different conformations. Nat Med 4:1157–1165.

Shmerling D, Hegyi I, Fischer M, Blättler T, Brandner S, Götz J, Rülicke T, Flechsig E, Cozzio A, von Mering C, Hangartner C, Aguzzi A, Weissmann C (1998) Expression of amino-terminally truncated PrP in the mouse leading to ataxia and specific cerebellar lesions. Cell 93:203–214.

Shyng SL, Moulder KL, Lesko A, Harris DA (1995) The N-terminal domain of a glycolipid-anchored prion protein is essential for its endocytosis via clathrin-coated pits. J Biol Chem 270:14793–14800.

Solforosi L, Criado JR, McGavern DB, Wirz S, Sanchez-Alavez M, Sugama S, DeGiorgio LA, Volpe BT, Wiseman E, Abalos G, Masliah E, Gilden D, Oldstone MB, Conti B, Williamson RA (2004) Cross-linking cellular prion protein triggers neuronal apoptosis *in vivo*. Science 303:1514–1516.

Stewart RS, Harris DA (2001) Most pathogenic mutations do not alter the membrane topology of the prion protein. J Biol Chem 276:2212–2220.

Stewart RS, Harris DA (2003) Mutational analysis of topological determinants in prion protein (PrP) and measurement of transmembrane and cytosolic PrP during prion infection. J Biol Chem 278:45960–45968.

Stewart RS, Harris DA (2005) A transmembrane form of the prion protein is localized in the Golgi apparatus of neurons. J Biol Chem, in press.

Stewart RS, Drisaldi B, Harris DA (2001) A transmembrane form of the prion protein contains an uncleaved signal peptide and is retained in the endoplasmic reticulum. Mol Biol Cell 12:881–889.

Weissmann C (2004) The state of the prion. Nat Rev Microbiol 2:861–871.

Zanusso G, Liu D, Ferrari S, Hegyi I, Yin X, Aguzzi A, Hornemann S, Liemann S, Glockshuber R, Manson JC, Brown P, Petersen RB, Gambetti P, Sy MS (1998) Prion protein expression in different species: analysis with a panel of new mAbs. Proc Natl Acad Sci USA 95:8812–8816.

THE JOURNAL OF BIOLOGICAL CHEMISTRY
Vol. 280, No. 16, Issue of April 22, pp. 15855–15864, 2005
Printed in U.S.A.

A Transmembrane Form of the Prion Protein Is Localized in the Golgi Apparatus of Neurons*

Received for publication, October 29, 2004, and in revised form, January 10, 2005
Published, JBC Papers in Press, January 25, 2005, DOI 10.1074/jbc.M412298200

Richard S. Stewart and David A. Harris‡

From the Department of Cell Biology and Physiology, Washington University School of Medicine, St. Louis, Missouri 63110

^{Ctm}PrP is a transmembrane version of the prion protein that has been proposed to be a neurotoxic intermediate underlying prion-induced pathogenesis. In previous studies, we found that PrP molecules carrying mutations in the N-terminal signal peptide (L9R) and the transmembrane domain (3AV) were synthesized exclusively in the ^{Ctm}PrP form in transfected cell lines. To characterize the properties of ^{Ctm}PrP in a neuronal setting, we have utilized cerebellar granule neurons cultured from Tg(L9R–3AV) mice that developed a fatal neurodegenerative illness. We found that about half of the L9R-3AV PrP synthesized in these neurons represents ^{Ctm}PrP, with the rest being ^{Sec}PrP, the glycolipid anchored form that does not span the membrane. Both forms contained an uncleaved signal peptide, and they are differentially glycosylated. ^{Sec}PrP was localized on the surface of neuronal processes. Most surprisingly, ^{Ctm}PrP was concentrated in the Golgi apparatus, rather in the endoplasmic reticulum as it is in transfected cell lines. Our study is the first to analyze the properties of ^{Ctm}PrP in a neuronal context, and our results suggest new hypotheses about how this form may exert its neurotoxic effects.

Prion diseases are fatal neurological disorders of humans and animals characterized by ataxia and neuronal degeneration (1). Unlike other neurodegenerative diseases, they can have an infectious as well as a sporadic or familial origin. Most cases are associated with the presence of PrP^{Sc},[1] a conformationally altered isoform of PrP^{C}, a cell surface glycoprotein of uncertain function that is expressed primarily in neurons of the brain and spinal cord. PrP^{C} is monomeric, protease-sensitive, and rich in α-helical structure. In contrast, PrP^{Sc} is aggregated, protease-resistant, and rich in β-sheets. There is considerable evidence that PrP^{Sc} is an infectious protein and that conversion of PrP^{C} into PrP^{Sc} is the central event in the propagation of prions, the infectious agents in these diseases (2, 3).

Although it is clear that PrP^{Sc} accumulates in the brain during most prion diseases, there is uncertainty about the mechanisms responsible for neuronal death. Several lines of evidence suggest that PrP^{Sc} is not toxic when it is presented to neurons externally (4, 5) and that conversion of PrP^{C} to PrP^{Sc} within neurons may generate toxic intermediates or by-products. However, there is debate about the identity of these neurotoxic species (6). Several alternative forms of PrP, distinct from both PrP^{C} and PrP^{Sc}, have been proposed as key pathogenic entities based on experiments in cell culture and transgenic mice. These include transmembrane PrP (7, 8), cytosolic PrP (9), protease-sensitive PrP^{Sc} (10), and $PG14^{spon}$ PrP (11).

This report focuses on transmembrane PrP. PrP is unusual because it can exist in several different topological forms that are generated during synthesis in the endoplasmic reticulum (ER). Most molecules assume the form designated ^{Sec}PrP, in which the polypeptide chain has been fully translocated into the ER lumen with its C terminus attached to the lipid bilayer by a glycosylphosphatidylinositol (GPI) anchor (12, 13). Under certain circumstances, however, the protein can adopt either of two opposite transmembrane orientations (designated ^{Ctm}PrP and ^{Ntm}PrP) in which a highly conserved stretch of hydrophobic amino acids in the middle of the sequence integrates into the membrane (7, 14–16). In ^{Ctm}PrP, the C terminus of the protein lies in the ER lumen, whereas in ^{Ntm}PrP, the N terminus is luminal. Mutations within and adjacent to the transmembrane domain that enhance its hydrophobicity increase the proportion of ^{Ctm}PrP (from <10% to 20–30% of the total PrP) (7, 8, 17). Some of these mutations (A117V and P105L) are associated with familial prion diseases, whereas others (3AV) are not seen in human patients.

Because the brains of patients with the A117V mutation do not contain conventional PrP27–30 (the protease-resistant core of PrP^{Sc}) (18), it was proposed that ^{Ctm}PrP, rather than PrP^{Sc}, is the proximal cause of neurodegeneration in this these and possibly other cases of prion disease (7, 8). Consistent with this hypothesis, transgenic mice expressing PrP with ^{Ctm}PrP-favoring mutations develop a spontaneous neurodegenerative illness that is similar to scrapie, but without detectable PrP^{Sc} (7). Based on these and other results, it was suggested that ^{Ctm}PrP is a key neurotoxic intermediate in both familial and infectious prion diseases and that the amount of this form can be increased directly by pathogenic mutations, or indirectly by accumulation of PrP^{Sc} (8). However, uncertainties remain about the role of ^{Ctm}PrP in prion diseases because of recent reports that ^{Ctm}PrP levels do not change significantly during scrapie infection (19) or as a result of most pathogenic mutations (17).

Our laboratory has been interested in investigating further the role of ^{Ctm}PrP in prion diseases. To this end, we have identified mutations that cause PrP to be synthesized exclu-

* This work was supported by Department of Defense Grant DAMD-03-0531 (to R. S. S.) and National Institutes of Health Grant NS35496 (to D. A. H.). The costs of publication of this article were defrayed in part by the payment of page charges. This article must therefore be hereby marked "*advertisement*" in accordance with 18 U.S.C. Section 1734 solely to indicate this fact.

‡ To whom correspondence should be addressed: Dept. of Cell Biology and Physiology, Washington University School of Medicine, 660 South Euclid Ave., St. Louis, MO 63110. Tel.: 314-362-4690; Fax: 314-747-0940; E-mail: dharris@cellbiology.wustl.edu.

[1] The abbreviations used are: PrP^{Sc}, scrapie isoform of prion protein; endo H, endoglycosidase H; ER, endoplasmic reticulum; GPI, glycosylphosphatidylinositol; PIPLC, phosphatidylinositol-specific phospholipase C; PK, proteinase K; PrP, prion protein; PrP^{C}, cellular isoform of PrP; WT, wild type; CHO, Chinese hamster ovary; BHK, baby hamster kidney; Tg, transgene; PNGase, peptide:*N*-glycosidase; PBS, phosphate-buffered saline; PDI, protein-disulfide isomerase.

sively with the ^{Ctm}PrP topology, thus facilitating analysis of this form in the absence of the other topological variants. We demonstrated that ^{Ctm}PrP has an uncleaved, N-terminal signal peptide (16) and that substitution of charged residues in the hydrophobic core of the signal sequence strongly favors synthesis of ^{Ctm}PrP (19). Combining one of these mutations (L9R) with a previously studied mutation in the transmembrane domain (3AV) resulted in a protein that was expressed entirely as ^{Ctm}PrP after *in vitro* translation and transfection of cultured cells (16). The presence of the L9R-3AV mutation caused a striking change in the subcellular distribution of PrP; the protein was no longer present on the plasma membrane like wild-type PrP but was instead concentrated in the ER of transfected CHO, BHK, and N2a cells (16). This result raised the possibility that the ER could be a potential site for the neurotoxic action of ^{Ctm}PrP.

To extend our studies to an *in vivo* setting, we have recently created transgenic mice expressing L9R-3AV PrP.[2] We found that these mice develop a fatal, ataxic neurological disorder accompanied by extensive degeneration of cerebellar granule neurons and hippocampal pyramidal cells. To our surprise, we found that this phenotype was strongly dependent on coexpression of endogenous, wild-type PrP. Here we have taken advantage of the availability of Tg(L9R-3AV) mice to study the cell biology and metabolism of ^{Ctm}PrP in neurons. We find that, in contrast to transfected cell lines, cultured neurons expressing transgenically encoded L9R-3AV localize ^{Ctm}PrP to the Golgi apparatus rather than to the ER. This observation dramatically changes our view of the possible cellular pathways that may be responsible for ^{Ctm}PrP-induced neurotoxicity.

EXPERIMENTAL PROCEDURES

Transgenic Mice—Engineering of Tg(L9R-3AV) mice is described elsewhere.[2] The experiments reported here were carried out using mice from the B line, but similar results were obtained using mice from the C line (data not shown). Mice were hemizygous for the transgene array, and were maintained on both *Prn-p*$^{+/+}$ and *Prn-p*$^{0/0}$ backgrounds. Tg(WT-E1)/*Prn-p*$^{0/0}$ and Tg(PG14-A2)/*Prn-p*$^{0/0}$ mice have been described previously (20).

Cerebellar Granule Cell Culture—Primary cultures from 5-day-old pups were performed as described previously (21). Dissociated cells were resuspended in CGN medium (basal medium Eagle's, 10% dialyzed fetal bovine serum, 25 mM KCl, 2 mM glutamine, 50 μg/ml gentamycin) and plated at a density of 500,000 cells/cm^2 in polylysine-coated plastic plates or 8-well glass chamber slides. Cells were used after 4–5 days in culture. Based on staining with cell type-specific marker proteins, these cultures typically contained >95% granule neurons, with the remainder of cells being fibroblasts and astrocytes.

Antibodies—The following anti-PrP antibodies were used for immunoprecipitation, immunofluorescence staining, or Western blotting: 8H4 and 8B4 (22); 3F4 (23); anti-SP (19); P45-66 (12).

Metabolic Labeling of Cultured Cells and Immunoprecipitation of PrP—Cerebellar granule cells were labeled with 100–500 μCi/ml of ^{35}S-Promix (Amersham Biosciences) in CGN medium lacking methionine, cysteine, and bovine serum and containing B27 vitamin supplement (Invitrogen). In some experiments, cells were chased in complete medium lacking radioactive methionine and cysteine, with or without PIPLC (1 unit/ml; purified from *Bacillus thuringiensis* as described by Shyng *et al.* (24)). Pulse-chase labeling of CHO cells was carried out as described previously (25).

Cells were lysed in 0.5% SDS, 50 mM Tris-HCl (pH 7.5), and immunoprecipitation of PrP was carried out as described previously (25). To treat PrP with glycosidases, protein was eluted from protein A-Sepharose beads by heating at 95 °C for 5 min in 0.1% SDS, 50 mM Tris-HCl (pH 6.7). The eluate was incubated for 1 h at 37 °C with endo H, neuraminidase, or PNGase F (all from New England Biolabs, Beverly, MA) according to the manufacturer's directions. Immunoprecipitated PrP was analyzed by SDS-PAGE and autoradiography.

PrP Membrane Topology Assay—Cerebellar granule cells were metabolically labeled for 4–6 h as described above. Cells were then scraped into PBS, spun at 2,000 × *g* for 5 min, and resuspended in ice-cold homogenization buffer (250 mM sucrose, 5 mM KCl, 5 mM $MgCl_2$, 50 mM Tris-HCl (pH 7.5)). Cells were lysed by 12 passages through silastic tubing (0.3-mm inner diameter) connecting two syringes with 27-gauge needles, and nuclei were removed by centrifugation at 5,000 × *g* for 10 min. Aliquots of the postnuclear supernatant were diluted into 50 mM Tris-HCl (pH 7.5) and incubated for 60 min at 4 °C with 250 μg/ml PK in the presence or absence of 0.5% Triton X-100. Digestion was terminated by addition of phenylmethylsulfonyl fluoride (5 mM final concentration), and PrP was then immunoprecipitated and deglycosylated by treatment with PNGase F.

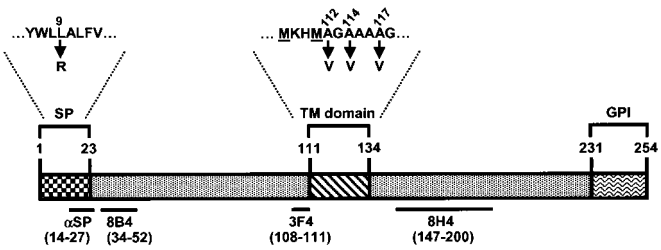

FIG. 1. **Schematic structure of mouse PrP.** *SP*, signal peptide; *TM*, transmembrane; *GPI*, glycosylphosphatidylinositol anchor addition sequence. The numbers *above* the drawing are the amino acid positions that define the ends of each domain. The *horizontal lines below* the drawing indicate the locations of epitopes recognized by antibodies used in this study, with the amino acid positions of each epitope given in *parentheses.* The amino acid sequence surrounding the L9R and 3AV mutations are shown *above* the signal peptide and transmembrane domains, respectively. 3AV is the designation for the triple mutation A112V/A114V/A117V. The *two underlined* methionine residues at positions 108 and 111 were introduced to create an epitope for 3F4 antibody, which allows discrimination of transgenically encoded and endogenous PrP.

Western Blotting—Brain tissue was homogenized using a Teflon pestle in 10 volumes of PBS containing protease inhibitors (phenylmethylsulfonyl fluoride, 20 μg/ml; leupeptin and pepstatin, 10 μg/ml). Homogenates were clarified by centrifugation at 2,000 × *g* for 5 min. Cultured neurons were lysed in 0.5% SDS, 50 mM Tris-HCl (pH 7.5), and the lysates were heated at 95 °C for 10 min. Protein was quantified using a BCA Assay (Pierce). Samples were analyzed by SDS-PAGE followed by immunoblotting with anti-PrP antibodies. In some cases, samples were treated with endo H or PNGase F, and proteins were recovered by methanol precipitation prior to SDS-PAGE.

Immunocytochemistry—Cerebellar granules cells were grown in 8-well chamber slides. For surface staining, cells were transferred to B27 medium (Dulbecco's modified Eagle's medium containing B27 vitamin supplement) and stained with anti-PrP antibodies (1:500 dilution) for 10 min at 37 °C. After rinsing in PBS, cells were fixed for 10 min at room temperature in 4% paraformaldehyde, 5% sucrose in PBS, blocked for 10 min in PBS, 2% goat serum, and stained with Alexa 488-conjugated goat anti-mouse IgG (Molecular Probes, Eugene, OR). Cells were mounted in 50% glycerol/PBS. In some cases, cells were incubated at 37 °C for 2 h with PIPLC (1 unit/ml) in B27 medium prior to fixation.

For visualization of intracellular PrP, cells were first fixed for 10 min at 4 °C in 4% paraformaldehyde, 5% sucrose in PBS and were then incubated for 10 min at 4 °C, either in 0.2% Triton X-100 in PBS (to permeabilize all membranes) or in 10 μg/ml digitonin in digitonin buffer (10% sucrose, 100 mM KOAc, 2.5 mM $MgCl_2$, 1 mM EDTA, 10 mM HEPES-HCl, pH 7.0) (to selectively permeabilize the plasma membrane) (26–28). After treatment with blocking solution, cells were stained with antibodies against PrP, giantin (Covance, Berkeley, CA), or PDI (StressGen, Victoria, British Columbia, Canada). Cells were then incubated with secondary antibodies (Alexa 488-conjugated goat anti-mouse IgG and Alexa 546-conjugated goat anti-rabbit IgG). In some experiments, cells were treated for 4 h with 10 μg/ml brefeldin A (Sigma) prior to staining. Cells were viewed with a Zeiss LSM 510 confocal microscope equipped with an Axiovert 200 laser scanning system.

RESULTS

The L9R-3AV mutation is illustrated in Fig. 1. We have generated and characterized two lines of transgenic mice that express PrP carrying this mutation.[2] These Tg(L9R-3AV) mice

[2] Stewart, R. S., Piccardo, P., Ghetti, B., and Harris, D. A. (2005) *J. Neurosci.*, in press.

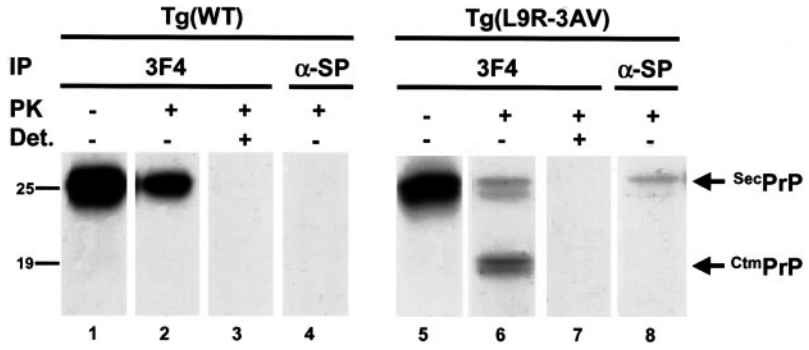

FIG. 2. **Neurons from Tg(L9R-3AV) mice produce both ^{Ctm}PrP and ^{Sec}PrP.** Cerebellar granule neurons cultured from Tg(WT) mice (*lanes 1–4*) or from Tg(L9R-3AV-B)/*Prn-p*$^{0/0}$ mice (*lanes 5–8*) were labeled for 4 h with [^{35}S]methionine. Postnuclear supernatants from all cultures were then incubated with (*lanes 2–4* and *6–8*) or without (*lanes 1* and *5*) PK in the presence (*lanes 3* and *7*) or absence (*lanes 1*, *2*, *4*, *5*, *6*, and *8*) of Triton X-100 (*Det.*). Proteins were then solubilized in SDS and enzymatically deglycosylated, and PrP was detected either by immunoprecipitation (*IP*) with either 3F4 antibody (*lanes 1–3* and *5–7*) or anti-SP antibody (*lanes 4* and *8*). The protease-protected forms of ^{Sec}PrP and ^{Ctm}PrP are indicated by *arrows to the right* of the gels. The protected bands appear as doublets in some samples due to nibbling of the polypeptide chain by PK. Molecular size markers are in kilodaltons.

develop a spontaneous neurological disorder characterized by ataxia and by loss of cerebellar granule cells and hippocampal pyramidal neurons. We utilized primary cultures of granule cells prepared from the cerebella of Tg(L9R-3AV) mice at postnatal day 5 to characterize the cell biology and metabolism of the mutant PrP in a neuronal setting.

Cultured Neurons from Tg(L9R-3AV) Mice Produce Both ^{Ctm}PrP and ^{Sec}PrP—We first used a protease protection assay to analyze the topology of L9R-3AV PrP in microsomes from granule neurons. Microsomes in a postnuclear supernatant prepared from [^{35}S]methionine-labeled neurons were subjected to digestion with proteinase K (PK), and PrP was then immunoprecipitated with 3F4 antibody after enzymatic deglycosylation (Fig. 2). We observed the following two protease-protected forms of PrP in approximately equal amounts (Fig. 2, *lane 6*): a 27-kDa band representing ^{Sec}PrP molecules that were fully protected from digestion because of their localization in the microsome lumen, and a 19-kDa fragment representing the luminal and transmembrane domains of ^{Ctm}PrP with the exposed cytoplasmic domain removed. We did not detect a 15-kDa fragment indicative of ^{Ntm}PrP. As expected, inclusion of Triton X-100 during protease treatment in order to disrupt microsomal membranes resulted in complete digestion of PrP (Fig. 2, *lane 7*). When the same analysis was carried out on microsomes from Tg(WT) neurons, only a fully protected 25-kDa band corresponding to ^{Sec}PrP was observed (Fig. 2, *lane 2*). Thus, granule neurons produce approximately equal proportions of ^{Sec}PrP and ^{Ctm}PrP from PrP carrying the L9R-3AV mutation. For both wild-type and mutant proteins, there was a decrease in the total amount of protected PrP after PK treatment, an effect that we attribute to the presence of some inside-out and damaged microsomes and not to the presence of cytoplasmic PrP.

Biosynthesis and Turnover of Mutant PrP—We used pulse-chase labeling with [^{35}S]methionine to analyze the biosynthetic maturation and degradation of L9R-3AV PrP in cerebellar granule neurons (Fig. 3*A*). A portion of each cell lysate was incubated with endoglycosidase H (endo H) prior to immunoprecipitation of PrP in order to test whether the *N*-linked glycans had matured to an endo H-resistant state, a step that occurs as proteins transit the mid-Golgi apparatus. At the end of the 20-min pulse-labeling period, a single species of PrP with a molecular mass of 32 kDa was observed. This form was shifted to 27 kDa, the size of unglycosylated PrP, by treatment with endo H, indicating the presence of immature glycan chains. The 32-kDa species was converted into two glycoforms of 32 and 35 kDa over the next 20 min of chase. Both of these mature forms contained glycans that were endo H-resistant. The 32- and 35-kDa glycoforms both decayed with a half-life of ~2.5 h, similar to the half-life of wild-type PrP in granule neurons (25). These data suggest the existence of a single metabolic pool of L9R-3AV PrP in neurons, implying that the ^{Ctm}PrP and ^{Sec}PrP in these cells do not have markedly different kinetic properties.

For comparison, we also analyzed the biosynthesis of L9R-3AV PrP in transiently transfected CHO cells (Fig. 3*B*). In CHO cells, the mutant protein was initially synthesized as two species of 32 and 27 kDa. The 27-kDa form was not glycosylated, and the 32-kDa form was core-glycosylated, because it is sensitive to endo H. However, the 32-kDa form in CHO cells remained endo H-sensitive throughout the entire chase period, unlike the case for the glycosylated forms of L9R-3AV in granule neurons. These results indicate that, whereas the mutant protein is retained in a pre-Golgi compartment in CHO cells, it transits beyond the mid-Golgi in granule neurons. Despite these differences in glycosylation and cellular trafficking, L9R-3AV PrP in CHO cells decayed with a half-life (~2.5 h) that was similar to the one observed for this mutant in neurons (see above) and for wild-type PrP in CHO cells (25).

L9R-3AV PrP Retains an Uncleaved Signal Peptide—We demonstrated previously that ^{Ctm}PrP synthesized by *in vitro* translation or by expression in CHO cells contains an uncleaved N-terminal signal peptide (16). To determine whether L9R-3AV PrP in cerebellar granule neurons also has the same feature, we immunoprecipitated PrP from [^{35}S]methionine-labeled cultures using anti-SP, an antibody that specifically recognizes PrP molecules containing an intact signal peptide (19). Parallel samples were immunoprecipitated with 3F4 or 8H4 antibodies, which recognize PrP molecules regardless of the presence of the signal peptide (see Fig. 1 for the location of antibody epitopes). As an additional way of discriminating molecules with and without the signal peptide, proteins were enzymatically deglycosylated to permit detection of the small size difference between the two species (27 and 25 kDa for signal peptide bearing, and signal peptide-cleaved forms, respectively).

When cultures from Tg(L9R-3AV)/*Prn-p*$^{+/+}$ mice were analyzed, two bands (25 and 27 kDa) of approximately equal intensity could be resolved after immunoprecipitation with 8H4 antibody (Fig. 4, *lane 1*). However, only the larger band was recognized by 3F4 and anti-SP antibodies (Fig. 4, *lanes 2* and *3*). This result demonstrates that the 27-kDa form represents transgenically encoded PrP that contains the 3F4 epitope and has an intact signal peptide, whereas the 25-kDa form represents endogenous mouse PrP that lacks the 3F4 epitope and has a cleaved signal peptide. Because >90% of the PrP recog-

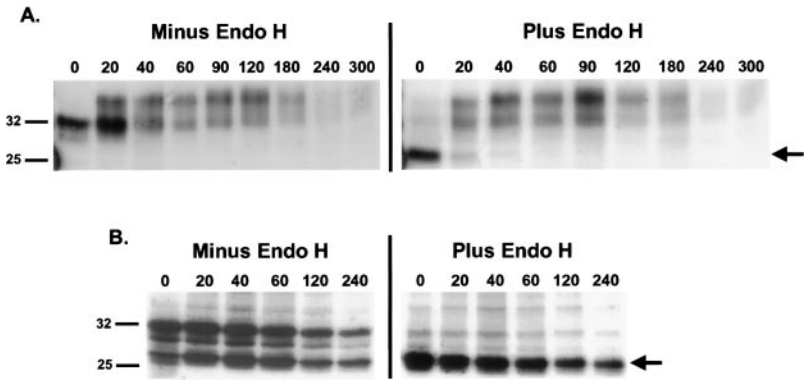

FIG. 3. **L9R-3AV PrP matures into an endo H-resistant form in cerebellar granule neurons but not in CHO cells.** *A*, cerebellar granule cells cultured from Tg(L9R-3AV-B)/*Prn-p*$^{+/+}$ mice were pulse-labeled with [^{35}S]methionine for 20 min and then chased for the indicated times (in min) in medium containing nonradioactive methionine. Cells were then lysed, and PrP was isolated by immunoprecipitation with 3F4 antibody. Half of the immunoprecipitated PrP was treated with endo H (gels on the *right*), and half was left untreated (gels on the *left*) prior to analysis by SDS-PAGE and autoradiography. The *arrow* at the *right* indicates the position of unglycosylated PrP. *B*, the same experiment as in *A* was performed on CHO cells transiently transfected with a plasmid encoding L9R-3AV PrP.

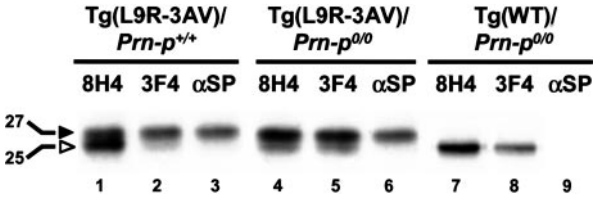

FIG. 4. **L9R-3AV PrP in neurons has an uncleaved signal peptide.** Cerebellar granule neurons from Tg(L9R-3AV-B)/*Prn-p*$^{+/+}$ mice (*lanes 1–3*), Tg(L9R-3AV-B)/*Prn-p*$^{0/0}$ mice (*lanes 4–6*), or Tg(WT)/*Prn-p*$^{0/0}$ mice (*lanes 7–9*) were labeled with [^{35}S]methionine for 4 h. PrP was then immunoprecipitated from cell lysates using either 8H4 (*lanes 1*, *4*, and *7*), 3F4 (*lanes 2*, *5*, and *8*), or anti-SP (*lanes 3*, *6*, and *9*) antibodies. Immunoprecipitated PrP was enzymatically deglycosylated with PNGase F prior to analysis by SDS-PAGE. The *filled* and *open arrowheads* to the *left* of *lane 1* indicate the signal peptide-bearing (27 kDa) and the signal peptide-cleaved (25 kDa) forms of PrP, respectively.

nized by 3F4 migrated at 27 kDa (*lane 2*), we infer that the majority of the L9R-3AV PrP in granule neurons, comprising both ^{Sec}PrP and ^{Ctm}PrP, retained an intact signal peptide. This conclusion was confirmed when we analyzed neurons from Tg(L9R-3AV)/*Prn-p*$^{0/0}$ mice. In this case, ~90% of the PrP immunoprecipitated by 3F4 migrated at 27 kDa, with the rest migrating at 25 kDa (Fig. 4, *lane 5*). A similar ratio of the two forms was observed with 8H4, the expected result because the neurons contain no endogenous PrP that would be recognized by this antibody (Fig. 4, *lane 4*). Again, only the 27-kDa form was immunoprecipitated by anti-SP (Fig. 4, *lane 6*). The amount of 25-kDa PrP in Tg(L9R-3AV) neurons varied somewhat in different experiments, possibly due to artifactual proteolysis after cell lysis, but it never exceeded ~20% of the total. As anticipated, Tg(WT) neurons produced only a 25-kDa form of PrP that was immunoprecipitated by 8H4 and 3F4 but not by anti-SP (Fig. 4*, lanes 7–9*).

Further evidence that ^{Sec}PrP contains an uncleaved signal peptide was provided by immunoprecipitation of PrP from PK-treated microsomes using anti-SP antibody (Fig. 2). The fully protected 27-kDa species in Tg(L9R-3AV) neurons reacted with anti-SP (Fig. 2, *lane 8*), whereas the corresponding 25-kDa band from Tg(WT) neurons did not (*lane 4*), implying that ^{Sec}PrP in the former cells contains an uncleaved signal peptide. As expected, the 19-kDa ^{Ctm}PrP fragment in Tg(L9R-3AV) neurons was not recognized by anti-SP (compare Fig. 2, *lanes 6* and *8*), because the N terminus of ^{Ctm}PrP lies on the cytoplasmic side of the membrane, and so its uncleaved signal peptide would be accessible to protease digestion.

^{Sec}PrP but Not ^{Ctm}PrP Is Present on the Neuronal Surface—In a previous study, we found by immunofluorescence staining that L9R-3AV PrP was absent from the surface of transfected CHO and BHK cells and was completely retained in the ER (16). This result was in accord with the observed endo H sensitivity of the protein in these cells. Our observation (Fig. 3) that L9R-3AV PrP in granule neurons matures to an endo H-resistant form suggested that localization of the mutant protein in these cells was likely to be different from CHO and BHK cells. We therefore analyzed the distribution of L9R-3AV PrP in granule neurons by using immunofluorescence microscopy.

In our first set of experiments, neurons from Tg(L9R-3AV)/*Prn-p*$^{0/0}$ mice were stained in the living state without permeabilization to selectively recognize PrP on the cell surface. As shown in Fig. 5, *A–C*, we observed positive staining with antibodies directed against three different epitopes distributed along the length of the PrP molecule (Fig. 1), including 8B4 (residues 34–52), 3F4 (residues 108–111), and 8H4 (residues 147–200). Staining was distributed along neuronal processes, which formed an extensive network throughout the culture. Because the epitopes for antibodies 8B4 and 3F4 are extracellular in ^{Sec}PrP but not in ^{Ctm}PrP, the accessibility of these epitopes to externally applied antibodies implied that at least some of the L9R-3AV PrP on the surface of the neurons must be in the ^{Sec}PrP form. Control experiments demonstrated that endogenous, wild-type PrP on neurons from *Prn-p*$^{+/0}$ mice stained with 8B4 and 8H4, but not with 3F4 (because endogenous PrP lacks the 3F4 epitope) (Fig. 5, *D–F*), and that none of the antibodies stained neurons from *Prn-p*$^{0/0}$ mice (not shown). In addition, neurons were not stained with an antibody directed against a cytoplasmic epitope of the Golgi protein, giantin, confirming the integrity of the surface membrane (not shown).

To further demonstrate the presence of ^{Sec}PrP on the cell surface, we treated living neurons with PIPLC, a bacterial enzyme which cleaves the C-terminal GPI anchor. PIPLC is predicted to release ^{Sec}PrP, but not ^{Ctm}PrP, from the cell surface, because the latter has a transmembrane segment that would maintain attachment to the plasma membrane even after the GPI anchor was cleaved. We found that PIPLC treatment eliminated virtually all surface staining for PrP, assayed by using 8H4 antibody, implying that most of the protein on the surface represented ^{Sec}PrP (Fig. 6, *A* and *D*). Any residual ^{Ctm}PrP should have reacted with 8H4, because the epitope recognized by this antibody is extracellular. As expected, wild-type PrP was also completely released by PIPLC from the surface of nontransgenic, *Prn-p*$^{+/+}$ neurons (Fig. 6, *B* and *E*). As an additional control, we demonstrated that neurons from Tg(PG14) mice did display residual PrP staining after PIPLC

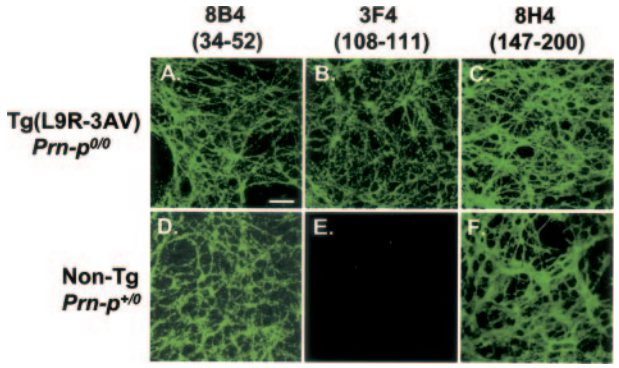

FIG. 5. **L9R-3AV PrP on the cell surface is accessible to antibodies recognizing epitopes distributed along the length of the molecule.** Cerebellar granule neurons cultured from Tg(L9R-3AV-B)/*Prn-p*$^{0/0}$ mice (*A–C*) or nontransgenic *Prn-p*$^{+/0}$ mice (*D–F*) were stained without permeabilization using antibodies 8B4 (*A* and *D*), 3F4 (*B* and *E*), or 8H4 (*C* and *F*) to reveal surface PrP. The epitopes recognized by each antibody are given in *parentheses*. The *scale bar* in *A* (applicable to all panels) is 25 μm.

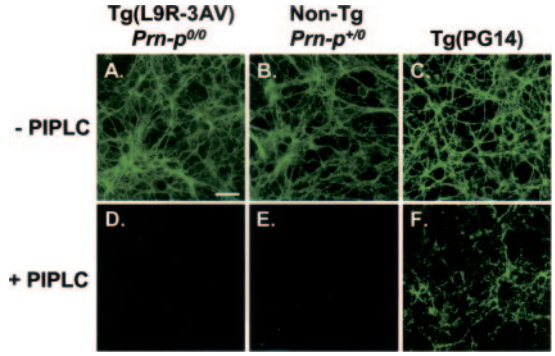

FIG. 6. **L9R-3AV PrP on the cell surface is releasable with PIPLC.** Cerebellar granule cells cultured from Tg(L9R-3AV-B)/*Prn-p*$^{0/0}$ mice (*A* and *D*), nontransgenic *Prn-p*$^{+/0}$ mice (*B* and *E*), or Tg(PG14) mice (*C* and *F*) were incubated with (*D–F*) or without (*A–C*) PIPLC and were then stained without permeabilization using anti-PrP antibodies. 8H4 antibody was used for *A*, *B*, *D*, and *E*; and 3F4 antibody was used for *C* and *F*. The *scale bar* in *A* (applicable to all panels) is 25 μm.

treatment, consistent with the partial resistance of the PG14 protein to GPI anchor cleavage (20) (Fig. 6, *C* and *F*). This control rules out the possibility that protease contamination in the PIPLC preparation degraded surface PrP. Taken together, our results indicate that there is little ^{Ctm}PrP on the cell surface and that most of the protein in this location represents ^{Sec}PrP.

^{Ctm}PrP Is Localized to the Golgi Apparatus—Because about half of the L9R-3AV PrP present in granule neurons represents ^{Ctm}PrP (Fig. 2), and because little of this form is present on the cell surface (Fig. 6), our results suggested that ^{Ctm}PrP was likely to be localized in an intracellular compartment. To visualize the intracellular distribution of the mutant protein, we stained neurons that had been permeabilized with Triton X-100. In control experiments with *Prn-p*$^{+/0}$ neurons, wild-type PrP was found to be localized primarily along neuronal processes (Fig. 7*A*), corresponding to the surface PrP visualized on these cells by staining without permeabilization (Fig. 5, *D* and *F*). The distribution of PrP in neurons from Tg(L9R-3AV) mice, on both *Prn-p*$^{0/0}$ and *Prn-p*$^{+/+}$ backgrounds, was markedly different. The mutant protein was concentrated in discrete, perinuclear structures in the soma that colocalized with the Golgi marker protein, giantin (Fig. 7, *D–F*). Staining of neuronal processes was less prominent in these permeabilized neurons than in unpermeabilized ones (compare Figs. 5*A* and 7*D*),

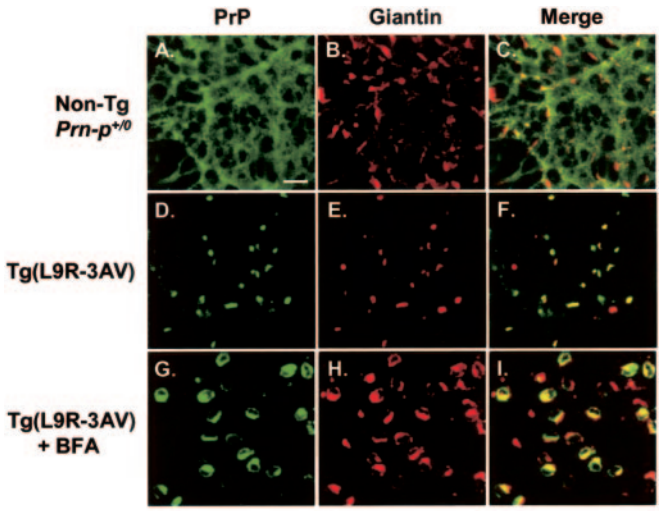

FIG. 7. **L9R-3AV PrP inside neurons is localized to the Golgi apparatus and is redistributed by brefeldin A (*BFA*).** Cerebellar granule cells cultured from nontransgenic *Prn-p*$^{+/0}$ mice (*A–C*) or from Tg(L9R-3AV-B)/*Prn-p*$^{0/0}$ mice (*D–I*) were fixed, permeabilized with Triton X-100, and then stained with anti-PrP and anti-giantin antibodies. Prior to fixation, one set of cultures (*G–I*) was treated with brefeldin A (10 μg/ml) for 4 h at 37 °C. A *green*-labeled secondary antibody was used to visualize PrP (*A*, *D*, and *G*), and a *red*-labeled secondary antibody was used to visualize giantin (*B*, *E*, and *H*). *C*, *F*, and *I* show a merged image of the green and red channels, demonstrating colocalization of PrP and giantin (*yellow*) in neurons from Tg(L9R-3AV) but not nontransgenic mice. Brefeldin A causes a redistribution of both PrP and giantin in Tg(L9R-3AV) neurons. 8H4 was used to stain PrP in *A* and 8B4 in *D* and *G*, but equivalent results were obtained regardless of which of these two antibodies was used (not shown). The *scale bar* in *A* (applicable to all panels) is 25 μm.

which reflects partial extraction of plasma membrane PrP as well as enhanced reactivity of cytoplasmic epitopes of Golgi-resident PrP after Triton X-100 treatment.[3] To confirm the Golgi localization of L9R-3AV PrP, we treated neurons with brefeldin A, which causes fusion of the ER and Golgi compartments. This treatment resulted in a redistribution of both PrP and giantin to a more diffuse pattern, consistent with the conclusion that the two proteins reside in the same structures (Fig. 7, *G–I*). We conclude from these results, and from the results with unpermeabilized cells (Figs. 5 and 6), that L9R-3AV PrP in neurons is present in the Golgi apparatus as well as on the plasma membrane.

We performed a series of experiments to directly probe the membrane topology of L9R-3AV PrP *in situ* by immunofluorescence staining. Treatment of cells with digitonin, a cholesterol-binding detergent, permeabilizes only the plasma membrane but not internal membranes such as those of the Golgi and ER, because the latter have a lower content of cholesterol (26–28). In contrast, Triton X-100 permeabilizes all membranes. We found that antibody 8B4, which is directed against an N-terminal epitope (Fig. 1, *34–52*), produced prominent Golgi staining in neurons permeabilized with either digitonin or Triton (Fig. 8, *A* and *E*). A similar result was seen with another N-terminally directed antibody, P45-66, which recognizes residues 45–66 within the octapeptide repeat region (not shown). In contrast, antibody 8H4, which reacts with a C-terminal region (Fig. 1, *147–200*), stained PrP in the Golgi only after Triton treatment (Fig. 8, *F–H*); in digitonin-treated neurons, staining was visible exclusively on neuronal processes, representing cell surface PrP molecules (Fig. 8, *B–D*). The observation that N-terminal epitopes of L9R-3AV PrP are accessible without permeabilization of Golgi membranes, whereas C-ter-

[3] R. S. Stewart and D. A. Harris, unpublished observations.

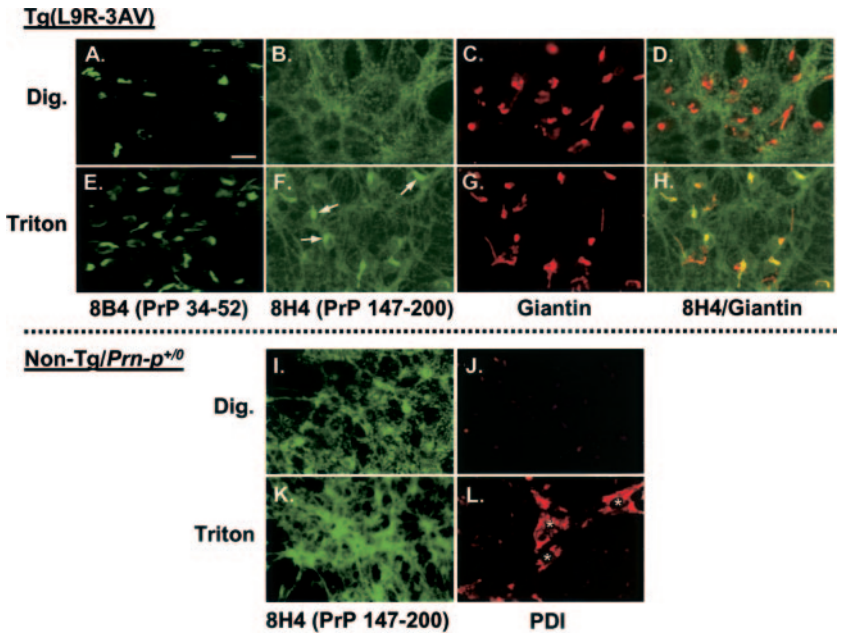

FIG. 8. **L9R-3AV PrP in the Golgi apparatus has the ^{Ctm}PrP topology.** Cerebellar granule cells cultured from Tg(L9R-3AV-B)/*Prn-p*$^{0/0}$ mice (*A–H*) or nontransgenic *Prn-p*$^{+/0}$ mice (*I–L*) were fixed and permeabilized with either digitonin (*Dig.*) (*A–D*, *I*, and *J*) or Triton X-100 (*E–H*, *K*, and *L*). Cells were then stained for PrP using either 8B4 (*A* and *E*) or 8H4 (*B*, *F*, *I*, and *K*) in conjunction with a green-labeled secondary antibody. Cells were simultaneously stained for a cytoplasmic epitope of giantin (*C* and *G*) or for PDI (*J* and *L*) in conjunction with a red-labeled secondary antibody. *D* and *H* show a merged image of the red and green channels. The *arrows* in *F* indicate spots of PrP staining that become apparent only after Triton permeabilization and that colocalize with giantin (*yellow* color in *H*). The *asterisks* in *L* indicate the location of fibroblasts in which PDI is visualized only after Triton permeabilization. The *scale bar* in *A* (applicable to all panels) is 25 μm.

minal epitopes are not, indicates that mutant protein in the Golgi has the ^{Ctm}PrP topology. When we performed the same experiment on neurons from nontransgenic *Prn-p*$^{+/0}$ mice, neurite staining was observed with both 8B4 and 8H4, regardless of the method of permeabilization (Fig. 8, *I* and *K*). This result reflects the fact that most wild-type PrP is found on the surface of neuronal processes, where it is present in the form of ^{Sec}PrP.

Two control experiments demonstrated the selectivity of the permeabilization procedures. Protein-disulfide isomerase (PDI), a luminal ER protein, was accessible to staining in Triton-treated but not digitonin-treated cultures, proving that digitonin did not permeabilize internal membranes. This result was most easily appreciated in the small number of fibroblasts present in the cultures, which have higher PDI levels than the neurons (Fig. 8, *J* and *L*). In contrast, an antibody to a cytoplasmic epitope of giantin stained the Golgi apparatus of neurons treated with either digitonin or Triton, demonstrating permeabilization of the plasma membrane by both detergents (Fig. 8, *C* and *G*).

Taken together, our immunofluorescence localization studies of intact and permeabilized neurons indicate that the ^{Ctm}PrP form L9R-3AV PrP is concentrated in the Golgi apparatus, whereas the ^{Sec}PrP form is present on the surface of neuronal processes like wild-type PrP.

^{Sec}PrP and ^{Ctm}PrP Are Differentially Glycosylated—We wondered whether the 32- and 35-kDa glycoforms of L9R-3AV PrP seen in pulse-labeling experiments (Fig. 3) might correspond to the two different topological forms of the protein, one being ^{Sec}PrP and the other, ^{Ctm}PrP. To answer this question, we treated [^{35}S]methionine-labeled neurons with PIPLC in order to release ^{Sec}PrP from the cell surface. We found that only the 32-kDa band was released into the medium by PIPLC, implying that this glycoform represents ^{Sec}PrP (Fig. 9*A*, *upper panels*). At least some of the 35-kDa glycoform that remained cell-associated after PIPLC treatment must therefore represent ^{Ctm}PrP. However, our results do not rule out the possibility that the 35-kDa band might also include molecules of ^{Sec}PrP that reside in intracellular compartments not accessible to externally applied PIPLC. In control experiments, wild-type PrP was completely released into the medium by PIPLC treatment, consistent with localization of virtually all of the protein on the cell surface (Fig. 9*A*, *lower panels*). In addition, both the 32- and 35-kDa glycoforms of L9R-3AV PrP underwent a characteristic decrease in gel mobility when detergent lysates were treated with PIPLC (Fig. 9*B*). Thus, lack of release of the 35-kDa form was due to its residence in an intracellular compartment, rather than to the presence of a phospholipase-resistant anchor structure.

To further analyze the glycoform profile of L9R-3AV in neurons, we tested the sensitivity of the oligosaccharide chains to neuraminidase, which cleaves sialic acid residues that are added in the trans cisterna of the Golgi. We found that both the 32- and 35-kDa forms of mutant PrP were shifted by neuraminidase treatment, although the shift was larger for the latter form (Fig. 9*C*, *lanes 2* and *3*). As observed previously, neither form was sensitive to endo H (Fig. 9*C*, *lane 4*). In contrast, both forms were shifted to 27 kDa, the size of unglycosylated PrP, by treatment with PNGase F, which cleaves all *N*-linked glycans regardless of structure (Fig. 9*C*, *lane 5*). These results indicate that both the 32- and 35-kDa forms of L9R-3AV PrP transit the trans cisterna of the Golgi in neurons but that the latter form is more heavily modified by sialic acid residues in that compartment. Consistent with an unusual oligosaccharide composition of the 35-kDa species is the fact that it has a higher M_r than mature, doubly glycosylated, wild-type PrP from cultured neurons, which migrates at 32 kDa (Fig. 9*C*, compare *lanes 1* and *2*).

Because our previous experiments were carried out on isolated cerebellar granule neurons, we also analyzed the glycosylation pattern of L9R-3AV PrP in whole brain by Western blotting. We found that the mutant protein in brain, as in cultured neurons, was composed of 32- and 35-kDa glycoforms, both of which were endo H-resistant and PNGase-sensitive

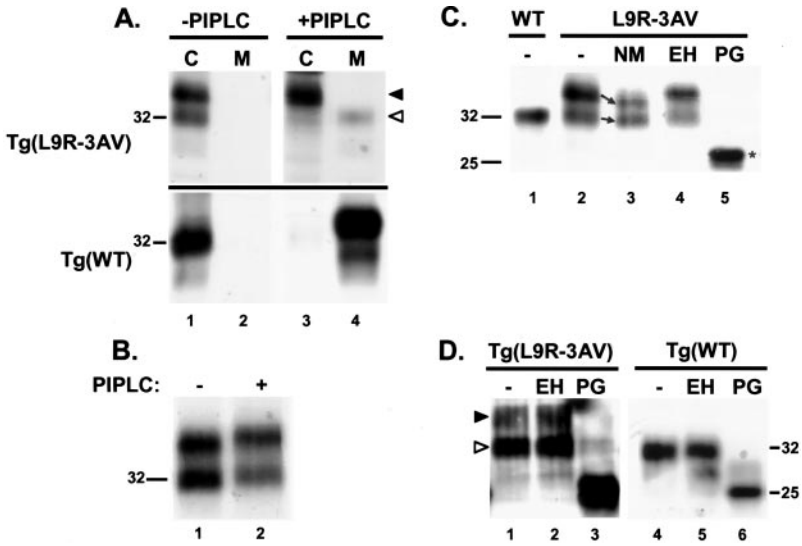

FIG. 9. **^{Sec}PrP and ^{Ctm}PrP are differentially glycosylated.** *A*, cerebellar granule cells cultured from Tg(L9R-3AV-B)/*Prn-p*$^{+/+}$ mice (*upper panels*) or from Tg(WT) mice (*lower panels*) were labeled for 3 h with [^{35}S]methionine and were then chased for 1.5 h in nonradioactive medium containing (*lanes 3* and *4*) or lacking (*lanes 1* and *2*) PIPLC. PrP in cells (*C*, *lanes 1* and *3*) and medium (*M*, *lanes 2* and *4*) was then immunoprecipitated with 3F4. Only the 32-kDa glycoform of L9R-3AV PrP (*open arrowhead*) is released into the medium by PIPLC, whereas the 35-kDa glycoform (*filled arrowhead*) remains cell-associated. Wild-type PrP is quantitatively released by PIPLC (*lower panel*, *lane 4*). *B*, cerebellar granule cells cultured from Tg(L9R-3AV-B)/*Prn-p*$^{+/+}$ mice were labeled and chased as in *A*. Cell lysates were incubated with (*lane 2*) or without (*lane 1*) PIPLC, and PrP was immunoprecipitated with 3F4. Note that both glycoforms undergo a small decrease in gel mobility. *C*, cerebellar granule cells cultured from Tg(WT) mice (*lane 1*) or from Tg(L9R-3AV-B)/*Prn-p*$^{+/+}$ mice (*lanes 2–5*) were labeled for 4 h with [^{35}S]methionine, and PrP was then immunoprecipitated from cell lysates using 3F4. Immunoprecipitated PrP was incubated without enzyme (*lanes 1* and *2*) or was treated with neuraminidase (*lane 3*), endo H (*lane 4*), or PNGase F (*lane 5*) prior to analysis by SDS-PAGE. The *arrows* between *lanes 2* and *3* indicate a shift in migration of the two glycoforms of L9R-3AV PrP following neuraminidase treatment. This shift is larger for the 35-kDa glycoform than for the 32-kDa glycoform (1.5 *versus* 1 kDa, respectively). The *asterisk* to the *right* of *lane 5* indicates the position of unglycosylated PrP. *WT*, wild type; *NM*, neuraminidase; *EH*, endo H; *PG*, PNGase F. *D,* homogenates of Tg(L9R-3AV) brain (*lanes 1–3*) or Tg(WT) brain (*lanes 4–6*) were Western-blotted by using 3F4 antibody. Samples were either left untreated (*lanes 1* and *4*) or were treated with endo H (*lanes 2* and *5*) or PNGase F (*lanes 3* and *6*). The *open* and *filled arrowheads* to the *left* of *lane 1* indicate the positions, respectively, of the 32- and 35-kDa glycoforms of L9R-3AV PrP.

(Fig. 9*D*, *lanes 1–3*). The proportion of the 35-kDa glycoform appeared to be lower in brain than in cultured neurons, but it was difficult to draw quantitative conclusions concerning the ratio of the two forms because of the weak reactivity of L9R-3AV PrP on Western blots.[2] In comparison, wild-type PrP in transgenic brain migrated as a major species of 32 kDa (Fig. 9*D*, *lane 4–6*). These results suggest that the post-translational processing of L9R-3AV PrP by isolated cerebellar granule neurons may be qualitatively similar to its processing by neurons *in situ* within transgenic brain.

DISCUSSION

We report here our analysis of PrP synthesized in cerebellar granule neurons cultured from Tg(L9R-3AV) mice. The PrP molecules in these cells carry an L9R-3AV mutation that strongly favors synthesis of ^{Ctm}PrP (16). Tg(L9R-3AV) mice develop a fatal neurological illness accompanied by extensive degeneration of several populations of neurons in the brain, including cerebellar granule cells.[2] Our results demonstrate that, in cerebellar granule neurons, ^{Ctm}PrP is concentrated in the Golgi apparatus, rather than in the ER as it is in transfected cells. Our study is the first to analyze the synthesis and subcellular localization of ^{Ctm}PrP in a neuronal context, and our results suggest new hypotheses about the mechanism by which this form may exert its neurotoxic effects.

Regulation of PrP Topology in Neurons—We found that granule neurons from Tg(L9R-3AV) mice express about 50% of the mutant protein as ^{Ctm}PrP and about 50% as ^{Sec}PrP. In contrast, we demonstrated previously that L9R-3AV PrP is synthesized almost exclusively with the ^{Ctm}PrP topology in transiently transfected CHO, BHK, and N2a cells (16). This difference between granule neurons and transfected cells may reflect the action of important regulatory mechanisms. The membrane topology of PrP is determined by sequence determinants in the polypeptide chain as well as by trans-acting factors that operate at the translocon during the translocation process (15, 29–31). ^{Ctm}PrP is the default topology of PrP synthesized in translocation reactions reconstituted from minimal components (Sec61p complex and SRP receptor) (31). Inclusion of an additional protein complex known as TRAP (translocon-associated protein) allows synthesis of ^{Sec}PrP as well as ^{Ctm}PrP in these reactions (32). One plausible explanation for our results is that the amount or activity of the TRAP complex, or of some other accessory factors, is different in granule neurons compared with transformed cell lines. It is also possible that, in conjunction with decreased capability for synthesis of ^{Ctm}PrP, neurons possess mechanisms for selectively degrading this form. This latter process may be important if neurons are particularly susceptible to a toxic effect of ^{Ctm}PrP.

^{Ctm}PrP and ^{Sec}PrP Are Differentially Localized—Our data demonstrate that ^{Sec}PrP is present on the plasma membrane, primarily on neuronal processes, whereas ^{Ctm}PrP is found in the Golgi apparatus in the cell body. This conclusion is based on immunofluorescence staining of cultured granule neurons and is consistent with the observed endo H resistance of L9R-3AV PrP in lysates of granule neurons and brain. We have also observed Golgi localization of L9R-3AV PrP in neurons by immunocytochemical staining of vibratome sections cut from the cerebellum, hippocampus, and cerebral cortex of Tg(L9R-3AV) mice, confirming the results reported here on granule neurons in culture.[2] Our data suggest the following model for the cellular trafficking of ^{Ctm}PrP and ^{Sec}PrP in neurons (Fig. 10). Both ^{Ctm}PrP and ^{Sec}PrP are initially synthesized in the ER and are then transported to the Golgi. ^{Ctm}PrP remains trapped

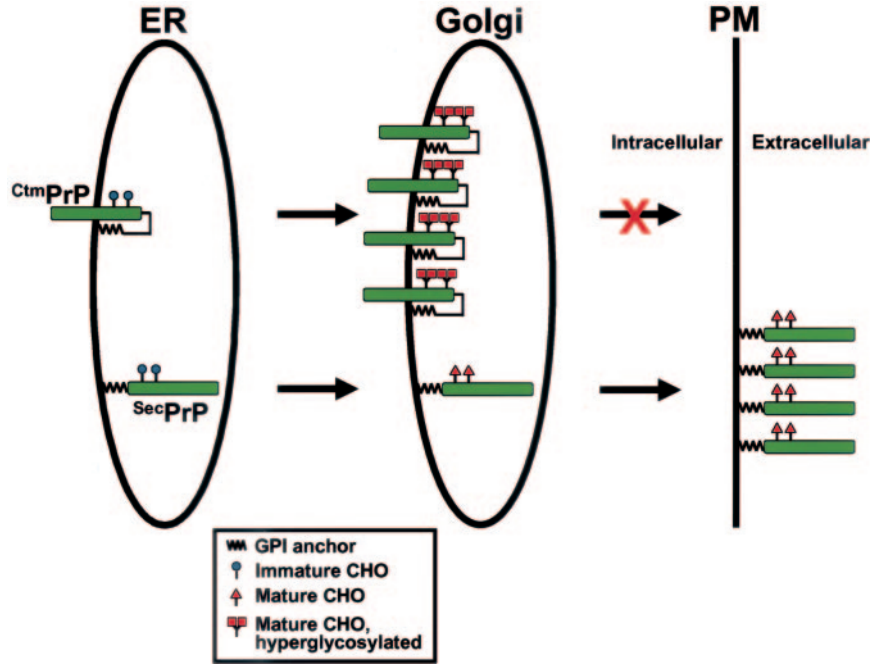

FIG. 10. **Model for the trafficking and glycosylation of ^{Ctm}PrP and ^{Sec}PrP in neurons based on analysis of L9R-3AV PrP.** *CHO*, *N*-linked oligosaccharide chain; *ER*, endoplasmic reticulum; *PM*, plasma membrane. Both ^{Ctm}PrP and ^{Sec}PrP are synthesized in the endoplasmic reticulum with immature (endo H-sensitive) oligosaccharide chains. Both forms are then transported to the Golgi where the oligosaccharide chains mature to an endo H-resistant form. ^{Ctm}PrP is retained in the Golgi where it becomes hyperglycosylated (35 kDa), and ^{Sec}PrP (32 kDa) continues along the secretory pathway to the plasma membrane.

in the Golgi, whereas ^{Sec}PrP continues its transit to the plasma membrane where it is eventually distributed along neuronal processes.

The explanation for the differential trafficking of ^{Ctm}PrP and ^{Sec}PrP remains to be determined. One possibility is that ^{Ctm}PrP contains a Golgi retention or retrieval signal that is absent in ^{Sec}PrP. The transmembrane domain of ^{Ctm}PrP is a likely candidate for such a retention signal, because a number of other Golgi resident proteins utilize membrane-embedded segments as retention signals (33). The L9R-3AV mutation itself does not seem to impair delivery of ^{Sec}PrP molecules to the cell surface, implying that this mutation does not result in gross misfolding of the protein.

The subcellular localization of L9R-3AV PrP in granule neurons is dramatically different from its localization in transiently transfected CHO, BHK, and N2a cells. In these transfected cells, the mutant protein is retained in the ER and remains endo H-sensitive throughout its metabolic lifetime (this paper and see Ref. 16). We have observed that L9R-3AV PrP is endo H-resistant in fibroblasts cultured from Tg(L9R-3AV) mice,[3] arguing that factors other than cell type determine the localization of the mutant protein. It is possible that the high expression levels characteristic of transiently transfected cells cause ER retention of ^{Ctm}PrP, whereas the more physiological levels present in cells from transgenic mice allow the protein to transit further along the secretory pathway.

Post-translational Processing of ^{Ctm}PrP and ^{Sec}PrP—Our pulse-chase labeling experiments indicate that L9R-3AV PrP is synthesized in the ER as an endo H-sensitive precursor that subsequently matures to two endo H-resistant glycoforms as the protein transits the Golgi. Our analysis indicates that these two glycoforms of 32 and 35 kDa correspond to ^{Sec}PrP and ^{Ctm}PrP, respectively. The 35-kDa form is larger than the mature, doubly glycosylated wild-type PrP (~32 kDa), and it undergoes a larger shift in gel mobility after treatment with neuraminidase. These observations suggest that ^{Ctm}PrP is hyperglycosylated, possibly due to its protracted residence in the Golgi apparatus, where sialic acids are added in the trans cisterna. Because the two glycoforms of mutant PrP migrate with different mobilities even after neuraminidase treatment, ^{Ctm}PrP must be distinguished from ^{Sec}PrP by post-translational modifications in addition to sialic acid residues. These conclusions regarding the maturation and glycosylation of ^{Ctm}PrP and ^{Sec}PrP have been incorporated into the model shown in Fig. 10.

Despite the difference in their subcellular localization and glycosylation, ^{Ctm}PrP and ^{Sec}PrP appear to decay with a similar metabolic half-life (~2.5 h). The mechanisms responsible for degradation of L9R-3AV in neurons and other cells remain to be determined. In a previous report, we showed by Western blotting that L9R-3AV PrP accumulated in transiently transfected BHK cells treated for 16 h with a proteasome inhibitor (16). This observation suggested that ^{Ctm}PrP may be a substrate for proteasomal degradation following retrotranslocation from the ER. However, we subsequently discovered that long term treatment of cells with proteasome inhibitors causes an artifactual increase in PrP mRNA levels when expression is driven from a strong viral promoter (25). When we tested shorter inhibitor treatments in pulse-chase labeling experiments, we found that the inhibitors had no effect on the maturation or turnover of L9R-3AV PrP in either cerebellar granule neurons or transfected cells.[3] We thus conclude that the proteasome does not play a prominent role in the metabolism of L9R-3AV PrP in these cell types.

The signal sequence of ^{Sec}PrP, like that of other secreted glycoproteins, is normally cleaved by a signal peptidase that acts in the lumen of the ER. In contrast, ^{Ctm}PrP contains an uncleaved signal sequence (16), reflecting the fact that the N terminus of this form remains in the cytoplasm and does not enter the ER lumen. We report here that, in neurons, both the Ctm and Sec forms of L9R-3AV PrP contain an uncleaved signal sequence, even though the latter molecules have been completely translocated into the ER lumen. One explanation for this phenomenon is that the L9R mutation itself interferes with the action of signal peptidase. Alternatively, signal peptidase may be less active, or the topogenesis of ^{Sec}PrP may be different, in neurons compared with non-neuronal systems. Analysis of L9R PrP expressed in neurons would help resolve this issue.

The presence of an uncleaved signal peptide does not seem to interfere with trafficking of mutant ^{Sec}PrP to the neuronal cell surface. Moreover, ^{Sec}PrP could be released from the cell surface by PIPLC, suggesting that the hydrophobic signal peptide does not integrate into the lipid bilayer. In pulse-chase exper-

iments (not shown), we found that L9R-3AV PrP molecules recognized by anti-SP antibody were present throughout the chase period and appeared to decay with a half-life similar to that of molecules recognized by 3F4 antibody. These results indicate that the mutant PrP in neurons is synthesized with an intact signal peptide and that the signal peptide is not selectively cleaved during maturation and turnover of the protein.

All of the experiments reported here have been carried out on cerebellar granule neurons cultured from Tg(L9R-3AV) mice. Of course, it is possible that other types of neurons may handle the mutant PrP differently. However, we find that Western blots of brain lysates from Tg(L9R-3AV) mice display the same endo H-resistant PrP glycoforms of 32 and 35 kDa that are seen in cultured granule neurons, albeit in different relative amounts. This result is consistent with the possibility that the post-translational processing and subcellular localization of mutant protein are qualitatively similar in many types of neurons in Tg(L9R-3AV) brain. This conclusion is also consistent with our observation that L9R-3AV PrP is concentrated in the Golgi of neurons from a number of brain regions, based on immunocytochemical staining of brain sections.[2]

Comparison with Other Studies—Ours is the first published study to examine the localization and metabolism of ^{Ctm}PrP in cultured neurons. Hegde *et al.* (7) have reported that PrP carrying either of two ^{Ctm}PrP-favoring mutations (3AV or K109I/H110I) is endo H-resistant in brain lysates from transgenic mice. This result implies that ^{Ctm}PrP induced by these mutations has also transited the mid-Golgi, although immunocytochemical localization studies would be necessary to confirm its precise localization.

Singh and colleagues have reported increased surface expression of a C-terminal fragment of ^{Ctm}PrP in neuroblastoma cells that have been treated with the synthetic peptide PrP106–126 (34), or that have been transfected to express another PrP mutant (P101L) (35). However, the fact that this fragment is releasable by treatment of cells with PIPLC calls into question its relationship to ^{Ctm}PrP.

Clues to the Neurotoxicity of ^{Ctm}PrP—Cerebellar granule neurons, as well as hippocampal pyramidal cells, undergo massive degeneration in the brains of Tg(L9R-3AV) mice. The localization of ^{Ctm}PrP in the Golgi apparatus of cerebellar granule neurons in culture raises the possibility that the toxic effects of ^{Ctm}PrP on this cell type *in vivo* may involve this organelle. Although apoptotic pathways are known to be triggered in the ER as a result of protein misfolding, the role of the Golgi in programmed cell death is less clear. The Golgi apparatus undergoes a dramatic disassembly process during apoptosis (36, 37). In addition, there are several caspase substrates and at least one procaspase and a caspase inhibitor that reside in this organelle. Thus, it is possible that ^{Ctm}PrP in the Golgi directly initiates apoptotic signals or amplifies signals that originate elsewhere in the cell. On the cell surface, PrP^{C} is known to be localized to lipid rafts that contain other GPI-anchored proteins (38, 39) and that have been implicated in several kinds of signaling pathways (40, 41). Because ^{Ctm}PrP contains a GPI anchor (16, 17), it is conceivable that this form is incorporated into lipid rafts that begin to assemble in the Golgi (40) and that this localization plays a role in neurotoxic signaling. Because the N-terminal half of the ^{Ctm}PrP molecule is cytoplasmic, interaction with pro-apoptotic proteins in the cytoplasm could play a role in the neurotoxic effects of ^{Ctm}PrP regardless of where along the secretory pathway this form is localized.

Most unexpectedly, we have found that the neurodegenerative phenotype in Tg(L9R-3AV) mice is strongly dependent on coexpression of endogenous, wild-type PrP.[2] For example, Tg(L9R–3AV-B$^{+/-}$)/*Prn-p*$^{+/+}$ mice develop neurological symptoms at ~170 days of age and die with extensive loss of cerebellar and hippocampal neurons at ~390 days of age. In contrast, mice from the same line on the *Prn-p*$^{0/0}$ background never develop symptoms and have histologically normal brains. These results imply that wild-type PrP^{C} influences the transmission of a toxic signal from ^{Ctm}PrP. We have shown in this study that the *Prn-p* status of the mice from which granule neurons are cultured has no effect on the topology ratio, subcellular localization, or post-translational processing of L9R-3AV PrP. Thus, endogenous PrP^{C} most likely influences the phenotype of the mice by altering the functional activity of ^{Ctm}PrP, rather than by changing its amount or distribution. We have postulated that wild-type ^{Sec}PrP normally mediates a neuroprotective signal that is converted to a toxic signal upon physical interaction with ^{Ctm}PrP.[2] This interaction may occur as ^{Sec}PrP transits the Golgi on its way to the cell surface. An important goal now will be the identification of the signaling pathways of which ^{Sec}PrP and ^{Ctm}PrP may be components. Neurons cultured from Tg(L9R-3AV) mice may prove crucial in these investigations.

Acknowledgments—We thank Richard Kascsak for 3F4 antibody, and Man-Sun Sy for 8H4 and 8B4 antibodies. We are grateful to Cheryl Adles and Michelle Kim for mouse colony maintenance and genotyping and to Leanne Stewart for assistance with neuronal culture techniques. We also thank Mike Green for a critical reading of the manuscript.

REFERENCES

1. Prusiner, S. B. (ed) (2004) *Prion Biology and Diseases*, 2nd Ed., Cold Spring Harbor Laboratory Press, Cold Spring Harbor, NY
2. Prusiner, S. B. (1998) *Proc. Natl. Acad. Sci. U. S. A.* **95,** 13363–13383
3. Weissmann, C. (2004) *Nat. Rev. Microbiol.* **2,** 861–871
4. Brandner, S., Isenmann, S., Raeber, A., Fischer, M., Sailer, A., Kobayashi, Y., Marino, S., Weissmann, C., and Aguzzi, A. (1996) *Nature* **379,** 339–343
5. Mallucci, G., Dickinson, A., Linehan, J., Klohn, P. C., Brandner, S., and Collinge, J. (2003) *Science* **302,** 871–874
6. Chiesa, R., and Harris, D. A. (2001) *Neurobiol. Dis.* **8,** 743–763
7. Hegde, R. S., Mastrianni, J. A., Scott, M. R., Defea, K. A., Tremblay, P., Torchia, M., DeArmond, S. J., Prusiner, S. B., and Lingappa, V. R. (1998) *Science* **279,** 827–834
8. Hegde, R. S., Tremblay, P., Groth, D., DeArmond, S. J., Prusiner, S. B., and Lingappa, V. R. (1999) *Nature* **402,** 822–826
9. Ma, J., Wollmann, R., and Lindquist, S. (2002) *Science* **298,** 1781–1785
10. Tremblay, P., Ball, H. L., Kaneko, K., Groth, D., Hegde, R. S., Cohen, F. E., DeArmond, S. J., Prusiner, S. B., and Safar, J. G. (2004) *J. Virol.* **78,** 2088–2099
11. Chiesa, R., Piccardo, P., Quaglio, E., Drisaldi, B., Si-Hoe, S. L., Takao, M., Ghetti, B., and Harris, D. A. (2003) *J. Virol.* **77,** 7611–7622
12. Lehmann, S., and Harris, D. A. (1995) *J. Biol. Chem.* **270,** 24589–24597
13. Stahl, N., Borchelt, D. R., and Prusiner, S. B. (1990) *Biochemistry* **29,** 5405–5412
14. Hölscher, C., Bach, U. C., and Dobberstein, B. (2001) *J. Biol. Chem.* **276,** 13388–13394
15. Kim, S. J., Rahbar, R., and Hegde, R. S. (2001) *J. Biol. Chem.* **276,** 26132–26140
16. Stewart, R. S., Drisaldi, B., and Harris, D. A. (2001) *Mol. Biol. Cell* **12,** 881–889
17. Stewart, R. S., and Harris, D. A. (2001) *J. Biol. Chem.* **276,** 2212–2220
18. Tateishi, J., Kitamoto, T., Doh-ura, K., Sakaki, Y., Steinmetz, G., Tranchant, C., Warter, J. M., and Heldt, N. (1990) *Neurology* **40,** 1578–1581
19. Stewart, R. S., and Harris, D. A. (2003) *J. Biol. Chem.* **278,** 45960–45968
20. Chiesa, R., Piccardo, P., Ghetti, B., and Harris, D. A. (1998) *Neuron* **21,** 1339–1351
21. Miller, T. M., and Johnson, E. M., Jr. (1996) *J. Neurosci.* **16,** 7487–7495
22. Zanusso, G., Liu, D., Ferrari, S., Hegyi, I., Yin, X., Aguzzi, A., Hornemann, S., Liemann, S., Glockshuber, R., Manson, J. C., Brown, P., Petersen, R. B., Gambetti, P., and Sy, M. S. (1998) *Proc. Natl. Acad. Sci. U. S. A.* **95,** 8812–8816
23. Bolton, D. C., Seligman, S. J., Bablanian, G., Windsor, D., Scala, L. J., Kim, K. S., Chen, C. M., Kascsak, R. J., and Bendheim, P. E. (1991) *J. Virol.* **65,** 3667–3675
24. Shyng, S. L., Moulder, K. L., Lesko, A., and Harris, D. A. (1995) *J. Biol. Chem.* **270,** 14793–14800
25. Drisaldi, B., Stewart, R. S., Adles, C., Stewart, L. R., Quaglio, E., Biasini, E., Fioriti, L., Chiesa, R., and Harris, D. A. (2003) *J. Biol. Chem.* **278,** 21732–21743
26. Otto, J. C., and Smith, W. L. (1994) *J. Biol. Chem.* **269,** 19868–19875
27. Kuroda, R., Kinoshita, J., Honsho, M., Mitoma, J., and Ito, A. (1996) *J. Biochem.* (*Tokyo*) **120,** 828–833
28. Eckhardt, M., Gotza, B., and Gerardy-Schahn, R. (1999) *J. Biol. Chem.* **274,** 8779–8787
29. Rutkowski, D. T., Lingappa, V. R., and Hegde, R. S. (2001) *Proc. Natl. Acad.*

Sci. U. S. A. **98,** 7823–7828
30. Kim, S. J., and Hegde, R. S. (2002) *Mol. Biol. Cell* **13,** 3775–3786
31. Hegde, R. S., Voigt, S., and Lingappa, V. R. (1998) *Mol. Cell* **2,** 85–91
32. Fons, R. D., Bogert, B. A., and Hegde, R. S. (2003) *J. Cell Biol.* **160,** 529–539
33. Colley, K. J. (1997) *Glycobiology* **7,** 1–13
34. Gu, Y., Fujioka, H., Mishra, R. S., Li, R., and Singh, N. (2002) *J. Biol. Chem.* **277,** 2275–2286
35. Mishra, R. S., Gu, Y., Bose, S., Verghese, S., Kalepu, S., and Singh, N. (2002) *J. Biol. Chem.* **277,** 24554–24561
36. Machamer, C. E. (2003) *Trends Cell Biol.* **13,** 279–281
37. Maag, R. S., Hicks, S. W., and Machamer, C. E. (2003) *Curr. Opin. Cell Biol.* **15,** 456–461
38. Vey, M., Pilkuhn, S., Wille, H., Nixon, R., DeArmond, S. J., Smart, E. J., Anderson, R. G. W., Taraboulos, A., and Prusiner, S. B. (1996) *Proc. Natl. Acad. Sci. U. S. A.* **93,** 14945–14949
39. Gorodinsky, A., and Harris, D. A. (1995) *J. Cell Biol.* **129,** 619–627
40. Brown, D. A., and London, E. (1998) *Annu. Rev. Cell Dev. Biol.* **14,** 111–136
41. Mouillet-Richard, S., Ermonval, M., Chebassier, C., Laplanche, J. L., Lehmann, S., Launay, J. M., and Kellermann, O. (2000) *Science* **289,** 1925–1928